Electronic Supplementary Material (ESI) for Organic Chemistry Frontiers.

SUPPORTING INFORMATION

Supramolecular Fluorescence Sensing of L-Proline and L-Pipecolic Acid

Andrés Felipe Sierra [a,b], Gemma Aragay [a], Guillem Peñuelas-Haro[a] and Pablo Ballester [a,c]*

[a] Institute of Chemical Research of Catalonia (ICIQ), The Barcelona Institute of Science and Technology (BIST), Avgda. Països Catalans 16, 43007 Tarragona, Spain

[b] Universitat Rovira i Virgili (URV), Departament de Química Analítica i Química Orgànica, c/Marcel·lí Domingo, 1, 43007 Tarragona, Spain

[c] ICREA, Passeig Lluís Companys 23, 08018 Barcelona, Spain

* Correspondence: pballester@iciq.es;

Contents

1 Materials and methods

All chemicals were purchased from commercial sources and used without further purification unless otherwise stated. Compounds **5in** and **5out** were synthesized following described procedures.[1] Pyrrole was distilled under vacuum and freshly used or stored in a freezer for further use. THF was dried from sodium/benzophenone and distilled under argon atmosphere. Triethylamine (Et_3N) was distilled from CaH_2 under argon atmosphere and was immediately used. Dried *N,N*-dimethylformamide was obtained from a solvent purification system M Braun SPS-800.

Flash column chromatography was performed with silica gel (technical grade, pore size 60 Å, 230-400 mesh particle size). Automatic column chromatography purifications were done with a Combi-flash® RF+. Analytical HPLC instrument consisted of an Agilent 1100 with autosampler and UV/vis detector using a Waters Spherisorb® (5.0 µm Silica, 4.6 mm × 250 mm) column and isocratic elution (DCM:AcOEt 90:10) (see SI for additional information).

Routine ^{1}H-NMR, ^{31}P-NMR and ^{13}C-NMR spectra were recorded on a Bruker Avance 400 (400 MHz for ^{1}H-NMR) or Bruker Avance 500 (500 MHz for ^{1}H-NMR) ultrashield spectrometer. Deuterated solvents were purchased from Aldrich. FT-IR measurements were carried out on a Bruker Optics FT-IR Alpha spectrometer equipped with a DTGS detector, KBr beamsplitter at 4 cm^{-1} resolution using a one bounce ATR accessory with diamond windows.

Solutions for optical spectroscopy studies were prepared in HPLC grade dichloromethane supplied by Scharlab, S.L.. UV-Vis measurements were carried out on a Shimadzu UV-2401PC spectrophotometer equipped with a photomultiplier detector, double beam optics and D2 and W light sources. Fluorescence measurements were carried out on a Fluorolog Horiba Jobin Yvon spectrofluorimeter equipped with photomultiplier detector, double monochromator and Xenon light source.

Energy minimized structures of the complexes were calculated at the BP86[2,3]/def2-SVP level of theory using Gaussian 09.[4]

2 Synthesis and characterization data

2.1 Synthesis of 6-(phenylamino)naphthalene-2-yl phosphonic dichloride (4)

The phosphonic acid dichloride **4** was synthesized following the procedure reported by Dalcanale *et al*.[5] The synthetic route is shown in Scheme S1.[111]

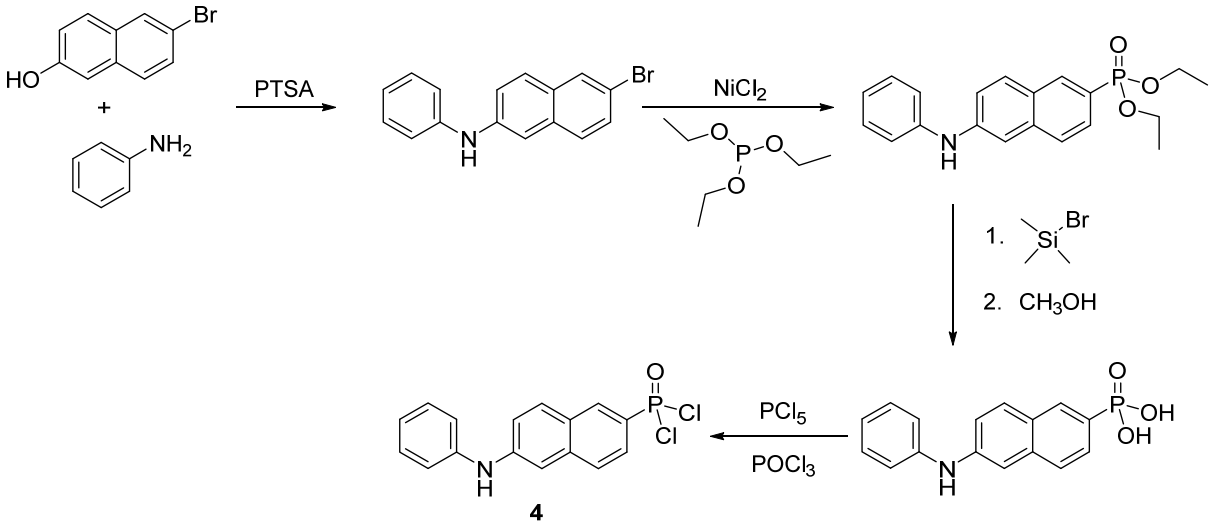

Scheme S1 Synthetic scheme for the synthesis of compound **4**.

2.2 Synthesis and separation of fluorescent receptors (1in and 1out)

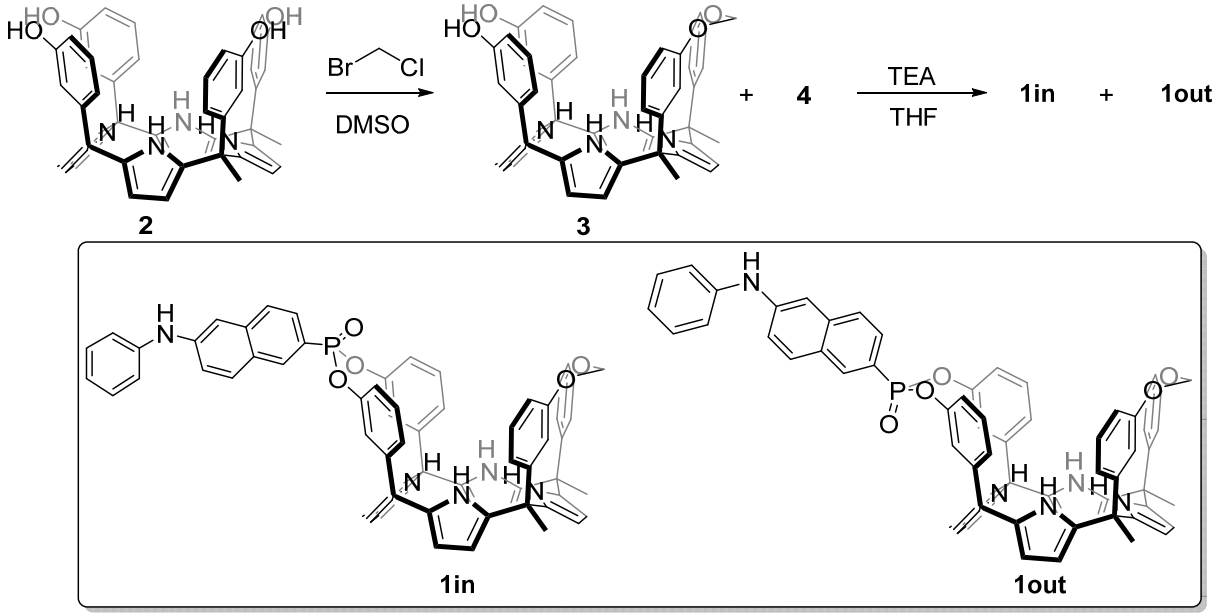

Scheme S2 Synthetic scheme for the synthesis of receptors **1in** and **1out.**

2.2.1 Synthesis of the mono-methylene bridged calix[4]pyrrole receptor (3)

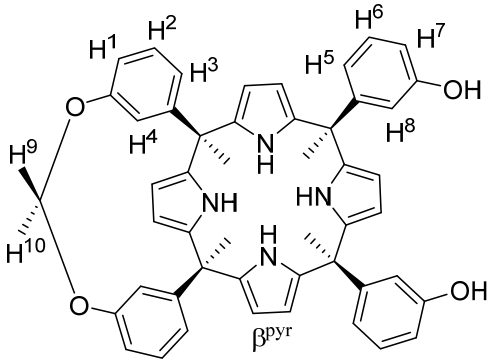

3

Synthesis of **3**: To an Ace pressure tube equipped with a magnetic stir bar and plunger valve, tetrol **2**[6] (1.50 g, 2.9025 mmol), and K_2CO_3 (2.24 g, 16.20 mmol, 8 equiv.) were added. The system was left under vacuum for one hour and then anhydrous DMSO (80 mL) was added under Ar atmosphere. To the resulting mixture, bromochloromethane (0.158 µl, 2.43 mmol, 1.2 equiv.) was added in one portion. The flask was sealed and heated overnight at 60 °C in an oil bath. The reaction mixture was then cooled down to RT and poured into 10% HCl(aq) (80 mL). The resulting suspension was extracted with DCM (3 × 50 mL). The organic portions were collected and washed with water (3 × 50 mL), dried over Na_2SO_4, filtered and evaporated under reduced pressure to yield a pale yellow powder (1.48 g). The final product was purified by combi-flash chromatography on a silica gel column (40 g silica column, DCM:AcOEt 90:10) to yield a white powder (800 mg). Finally, the white powder was further recrystallized in acetonitrile (5 ml) with some drops of DCM (720 mg, 48 % yield).

Receptor **3**. **Rf**: 0.5 (DCM:AcOEt 90:10, SiO_2) **Melting Point:** 255 °C. **^{1}H NMR** (500 MHz, $(CD_3)_2CO$, 298 K): δ (ppm) = 8.77 (bs, 2H, NH), 8.73 (bs, 1H, NH), 8.53 (bs, 1H, NH), 8.16 (s, 2H, OH), 7.07 (t, *J* = 7.85 Hz, 2H, H^2), 7.04 (t, *J* = 7.85 Hz, 2H, H^6), 6.79 (s, 2H, H^4), 6.70 (d, *J* = 8.02 Hz, 1H, H^1), 6.67 (dd, J_1 =8.02 Hz, J_2 = 1.92 Hz, 2H, H^3), 6.55 (dd, J_1 =8.02 Hz, J_2 = 1.92 Hz, 2H, H^5), 6.42 (d, *J* = 7.85 Hz, 2H, H^7), 6.38 (s, 2H, H^8), 6.36 (d, *J* = 8.25 Hz, 1H, H^9), 6.06 - 6.00 (m, 8H, $H^{\beta pyr}$), 5.33 (d, *J* = 8.25 Hz, 1H, H^{10}), 1.88 (s, 6H, CH_3), 1.84 (s, 6H, CH_3). **^{13}C NMR** (100 MHz, CD_2Cl_2, 298 K): δ (ppm) = 155.9, 154.9, 137.8, 137.7, 137.2, 136.7, 128.9, 128.8, 121.9, 120.4, 117.1, 116.9, 115.0, 113.3, 105.7, 105.1, 44.7, 44.6, 1.4.

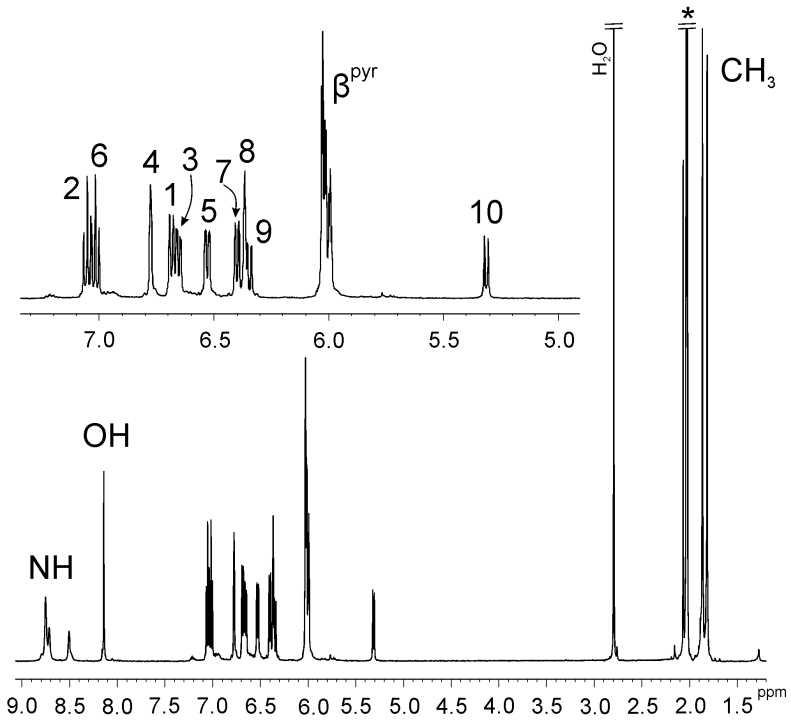

Figure S1 ^{1}H-NMR (500 MHz, $(CD_3)_2CO$, 298 K) of mono-methylene bridged calix[4]pyrrole **3**.*Residual solvent peak.

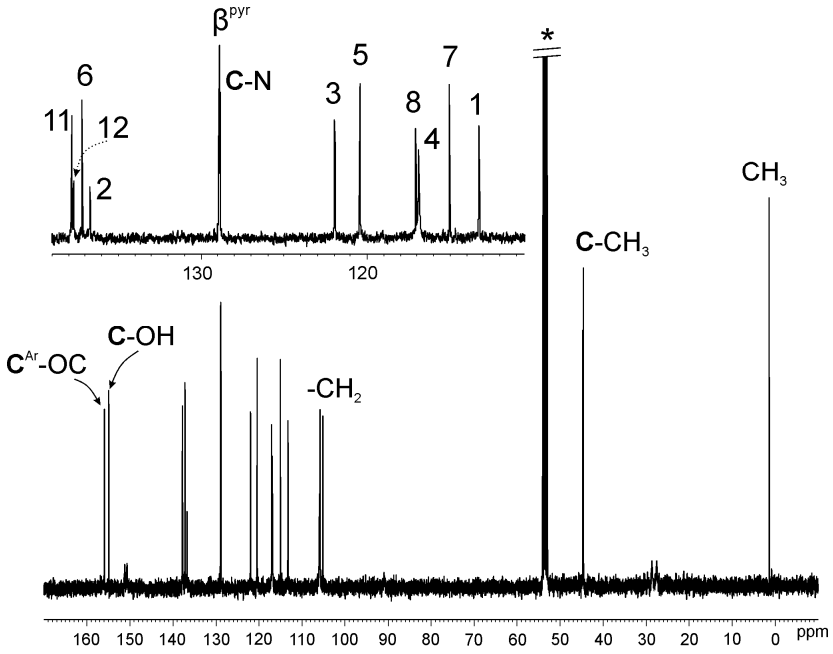

Figure S2 ^{13}C NMR (100 MHz, CD_2Cl_2, 298 K) of mono-methylene bridged calix[4]pyrrole **3**. *Residual solvent peak.

2.2.2 Synthesis of the mono-phosphonate calix[4]pyrrole cavitands 1in and 1out.

In a 25 mL Schlenk flask, compound **4** (180 mg, 0.535 mmol, 2.0 equiv.) was dried overnight under reduced pressure. Next day, the solid was dissolved on freshly dried THF (15 mL, 18 mM) and triethylamine (0.5 mL, 3.59 mmol, 13.5 equiv.) was added in one portion under Ar atmosphere. The mixture left under vigorous stirring for 15 min. This solution was added via cannula to a 5mL THF solution of mono-methylene bridged cavitand **3** (200 mg, 0.266 mmol, 1.0 equiv.) under Ar atmosphere.

The reaction was stirred at RT for 2 h. Then, the solvent was evaporated, and the resulting solid was solubilized in DCM (20 mL). The organic solution was washed with 10 mL of HCl (aq.) 10% and 10 mL of brine solution. Then, the aqueous phase was washed with DCM (2 × 20 mL). The organic portions were collected, dried over Na_2SO_4, filtered, and concentrated under reduced pressure yielding a pale brown solid (250 mg). The reaction produced a mixture of the two mono-phosphonate diastereoisomers **1in** and **1out**.

Conventional and combi-flash column chromatography purification proved to be not successful in the separation of the two diastereoisomers. Finally, analytical HPLC method was used for the diastereotopic separation of **1in** and **1out** (see next section for details).

2.2.3 Analytical HPLC separation of diastereoisomers 1in and 1out.

The reaction crude (after work-up) was passed through silica gel column chromatography as a pre-treatment using DCM as eluent. The collected combined fractions containing the desired products were analyzed by HPLC. After an optimization process, the elution mixture DCM/AcOEt 90:10 showed the best isomeric separation (**Figure S3**).

HPLC parameters:

Column: Waters Spherisorb® (5.0 µm Silica, 4.6 mm × 250 mm) column.

Mobile phase: DCM/AcOEt 90:10

Flux: 1 mL/min

Injection volume: 50 µL

Sample concentration: 1 mg/ml

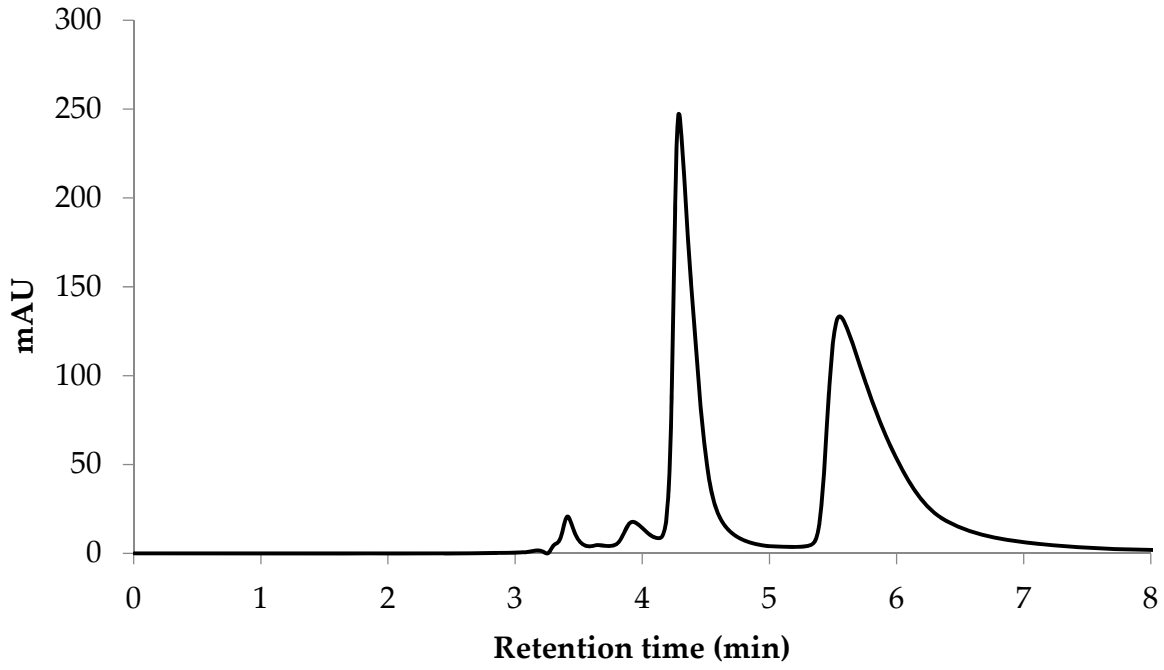

Figure S3 HPLC Chromatogram of the combined organic fractions containing receptors **1in** and **1out**.

After optimizing the analytical conditions, we performed a loading study using the same column and eluent mixture. We ran different injections (10 mg mL^{-1} in DCM) increasing the injection volume from 5 µL to 100 µL. The results from the loading study are shown in **Figure S4**.

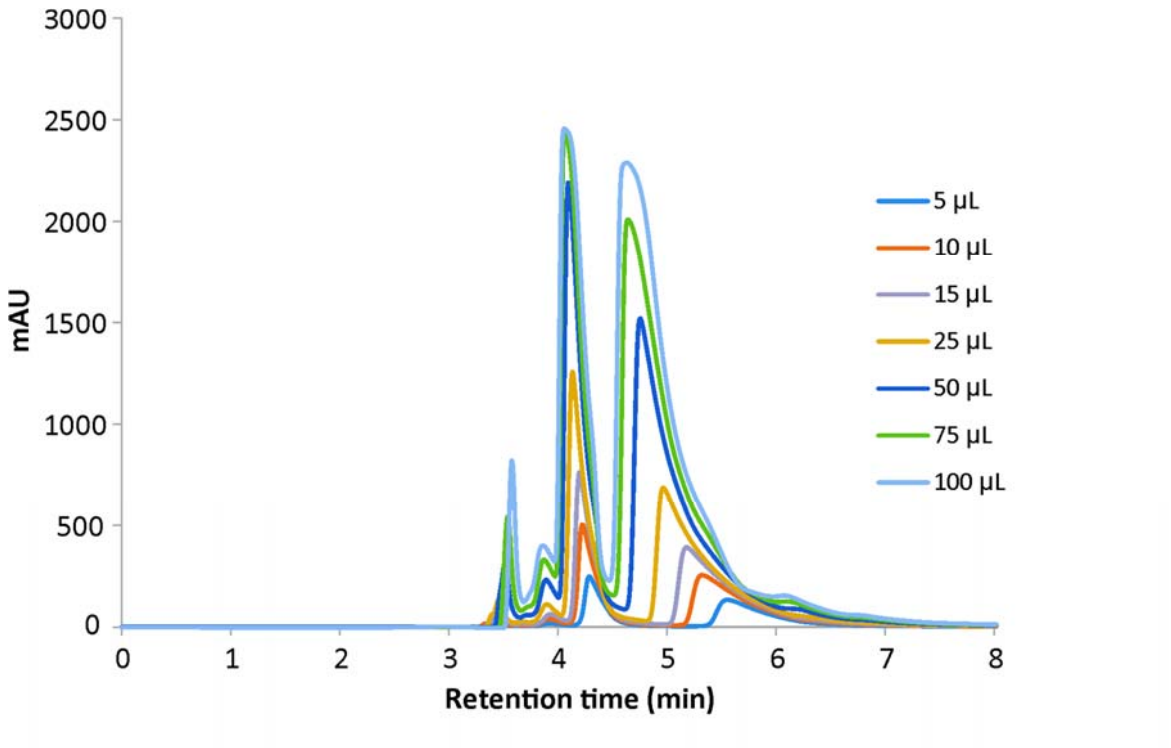

Figure S4 Stacked HPLC chromatograms obtained during the loading study of combined organic fractions containing receptors **1in** and **1out**.

Repetitive injections of the isomers' mixture (10 mg mL^{-1} in DCM) under the optimized conditions yielded 20 mg (15%) of each separated isomer. Crystals of **1in** and **1out** spontaneously grew in the NMR tubes from deuterated acetone or acetonitrile solutions. According to the X-ray diffraction results, the fraction with the shorter retention time (4.2 min) corresponded to the out isomer, while the fraction eluting later at 5 min corresponded to the **in** isomer.

Mono-phosphonate calix[4]pyrrole cavitand 1in

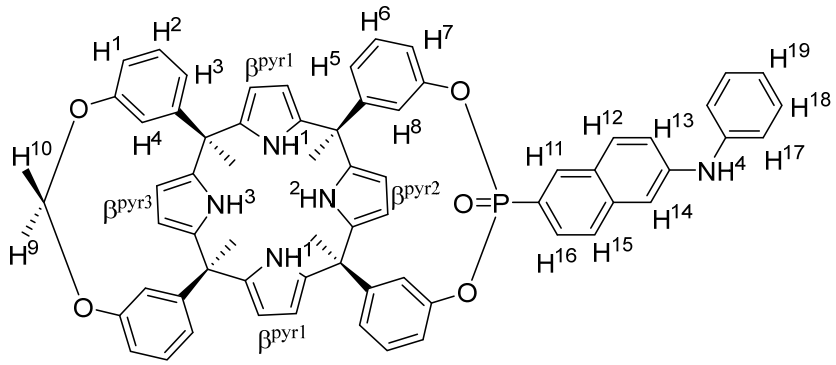

1in

Receptor **1in**. **Rf**: 0.3 (DCM:AcOEt 98:2, SiO_2). **^{1}H NMR** (400 MHz, $(CD_3)_2CO$, 298 K): δ (ppm) = 8.85 (bs, 2H, NH^1), 8.62 (bs, 1H, NH^2), 8.51 (bs, 1H, NH^3), 8.49 (d, 1H, H^{11}), 8.00 (d, 1H, *J* = 8.74 Hz, H^{12}), 7.98 (bs, 1H, NH^4), 7.93-7.83 (m, 2H, $H^{15,16}$), 7.58 (d, 1H, *J* = 2.20 Hz, H^{14}), 7.44 (dd, 1H, J_1 = 8.82 Hz, J_2 = 2.20 Hz, H^{13}), 7.39-7.31 (m, 4H, $H^{17,18}$), 7.22 (t, 2H, *J* = 7.87 Hz, H^6), 7.13 (t, 2H, *J* = 7.87 Hz, H^2), 7.06 (d, 2H, *J* = 8.05 Hz, H^7), 7.02 (tt, 1H, J_1 = 6.51 Hz, J_2 = 1.84 Hz, H^{19}), 6.85 (s, 2H, H^4), 6.82 (s, 2H, H^8), 6.83-6.78 (m, 4H, $H^{5,8}$), 6.72 (dd, 2H, J_1 = 8.10 Hz, J_2 = 1.30 Hz, H^1), 6.62 (d, 2H, *J* = 7.87 Hz, H^3), 6.44 (d, 1H, *J* = 8.06 Hz, H^9), 6.14 (d, 2H, *J* = 2.60 Hz, β^{pyr2}), 6.11 (d, 4H, *J* = 2.60 Hz, β^{pyr1}), 6.08 (d, 2H, *J* = 2.60 Hz, β^{pyr3}), 5.35 (d, 1H, *J* = 8.06 Hz, H^{10}), 1.91 (s, 6H, CH_3), 1.90 (s, 6H, CH_3). **^{31}P NMR** (161 MHz, $(CD_3)_2CO$, 298 K): δ (ppm) = 15.31.

Note: 2D-NMR experiments (COSY and ROESY) were used for the proton assignment of cavitand **1in** (**Figure S6** to **S11**)**.**

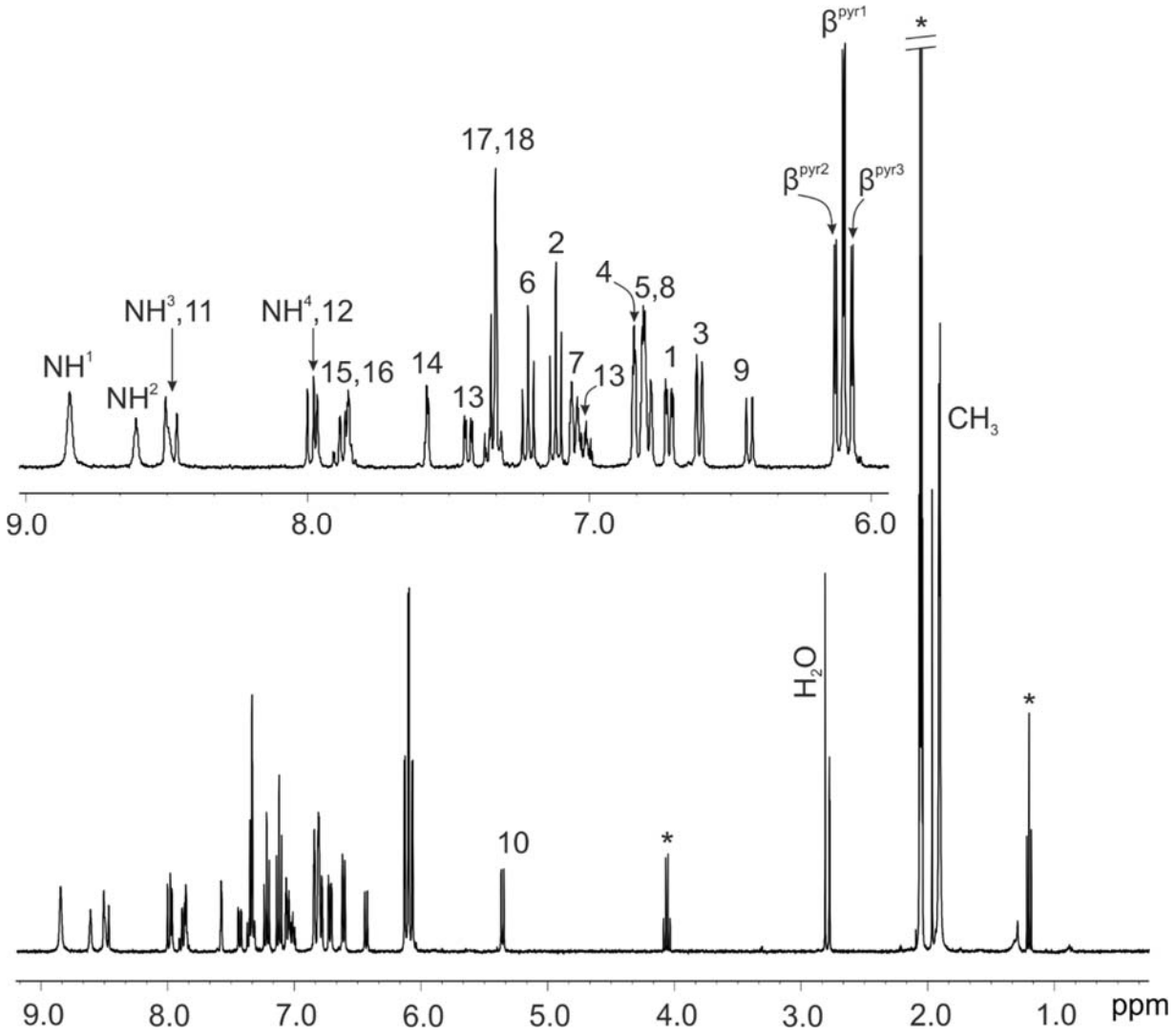

Figure S5 ^{1}H NMR (400 MHz, $(CD_3)_2CO$, 298 K) of **1in**. *Residual solvent peak.

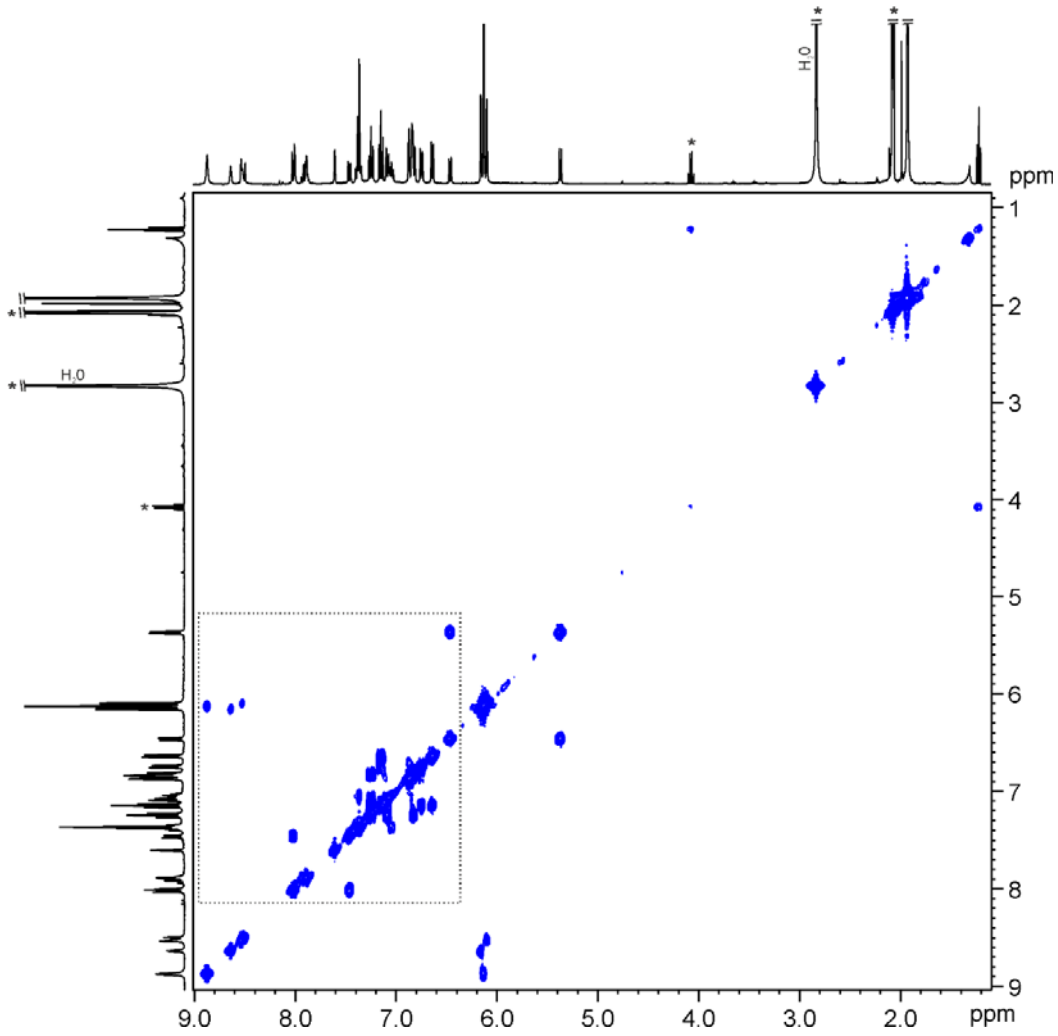

Figure S6 COSY NMR (400 MHz, $(CD_3)_2CO$, 298 K) spectrum of compound **1in**. * Residual solvent peak.

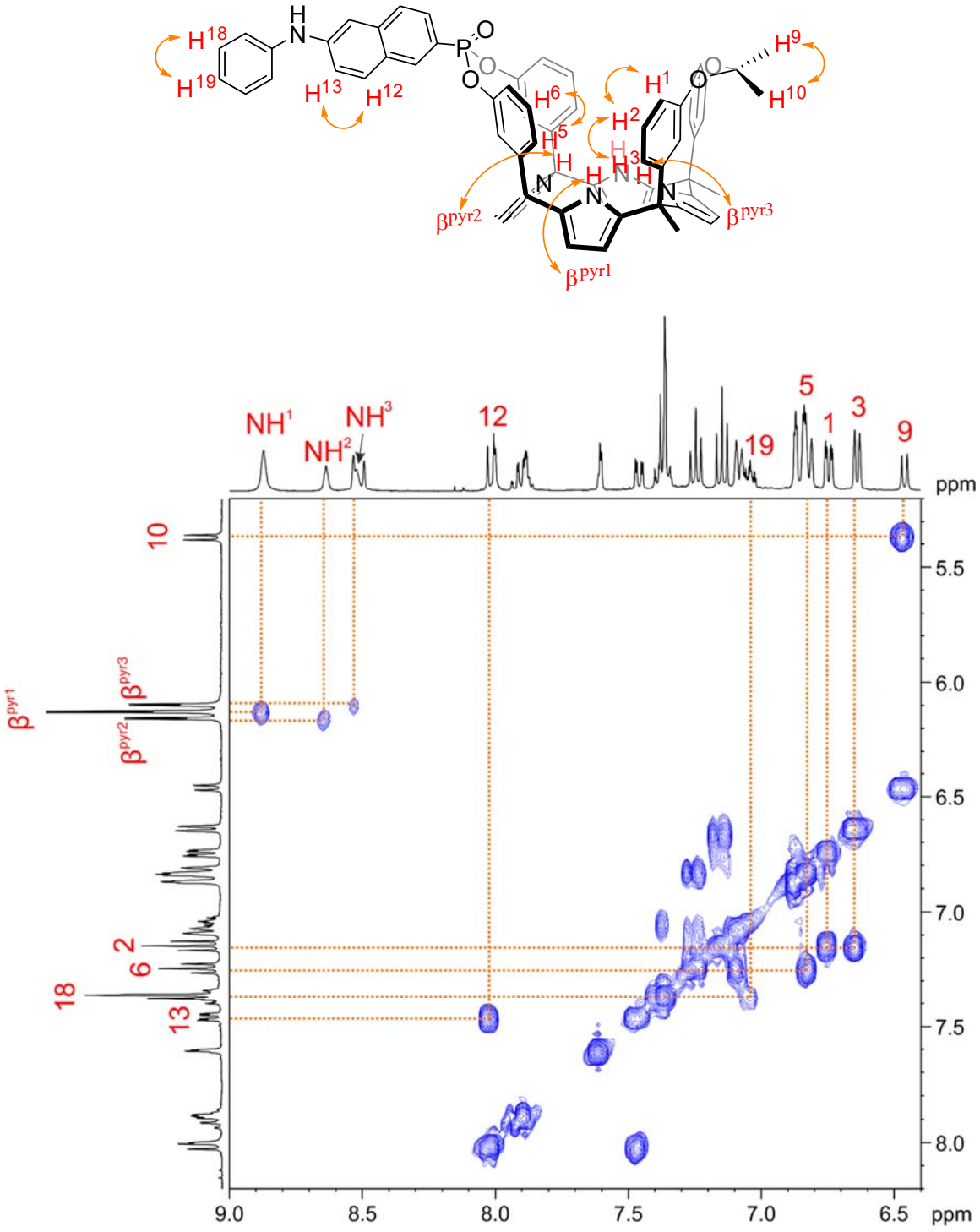

Figure S7 Selected region of the COSY NMR spectrum of the cavitand **1in**.

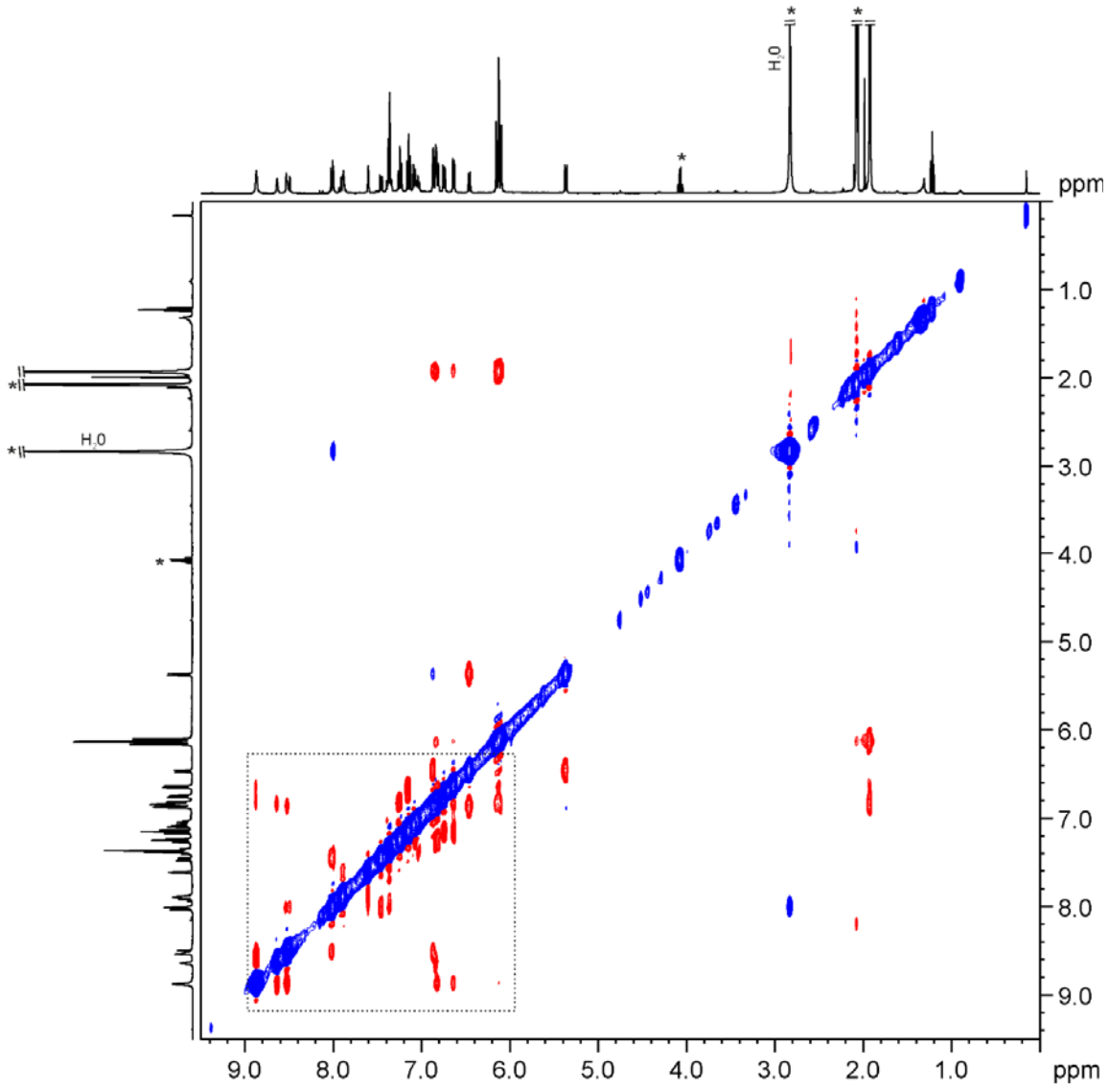

Figure S8 NOESY NMR (400 MHz, $(CD_3)_2CO$, 298 K) spectrum of cavitand **1in**. * Residual solvent peak.

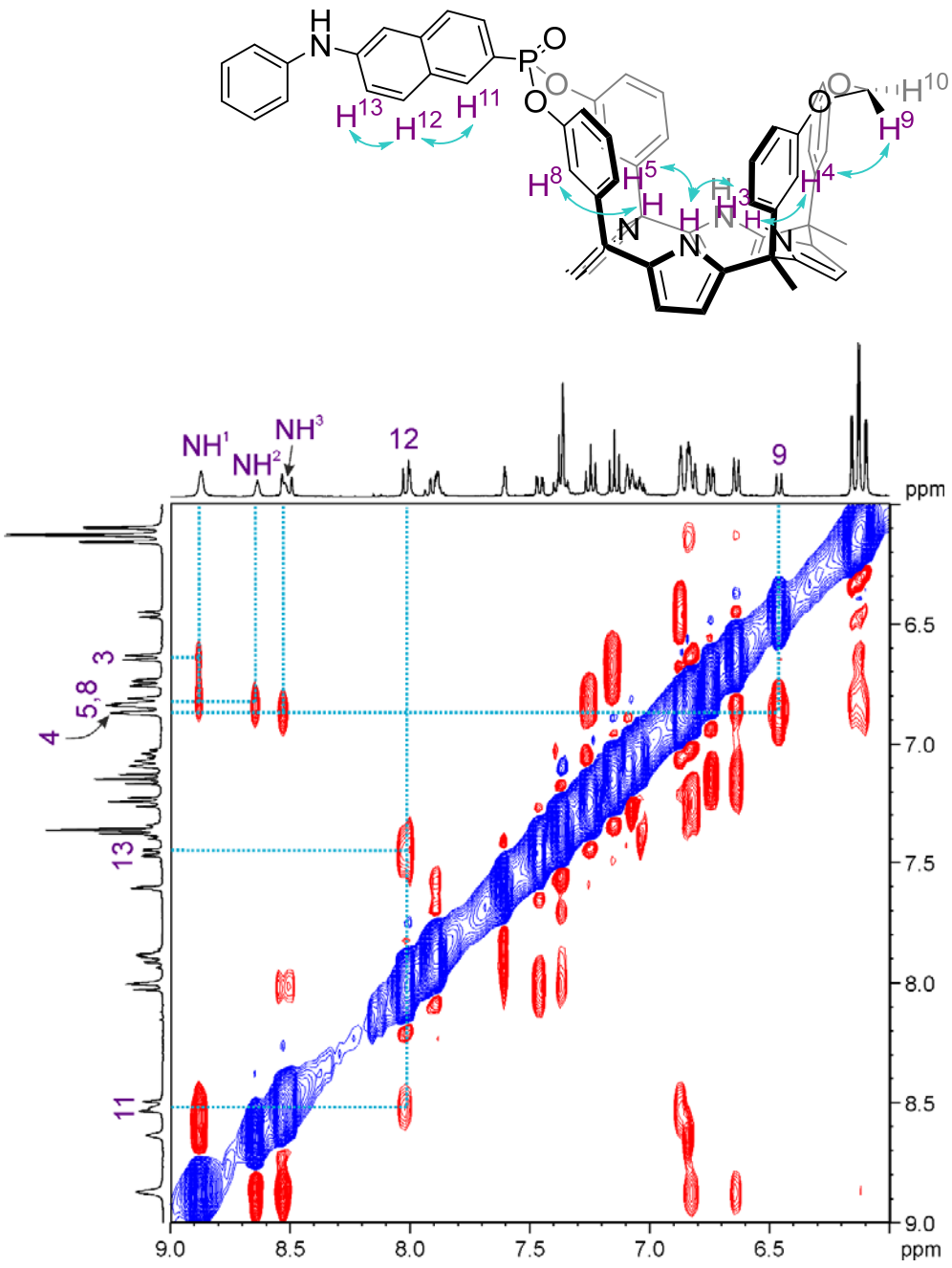

Figure S 9 Expansion of a selected region of the 2D NOESY NMR (400 MHz, $(CD_3)_2CO$, 298 K) spectrum of the cavitand **1in**.

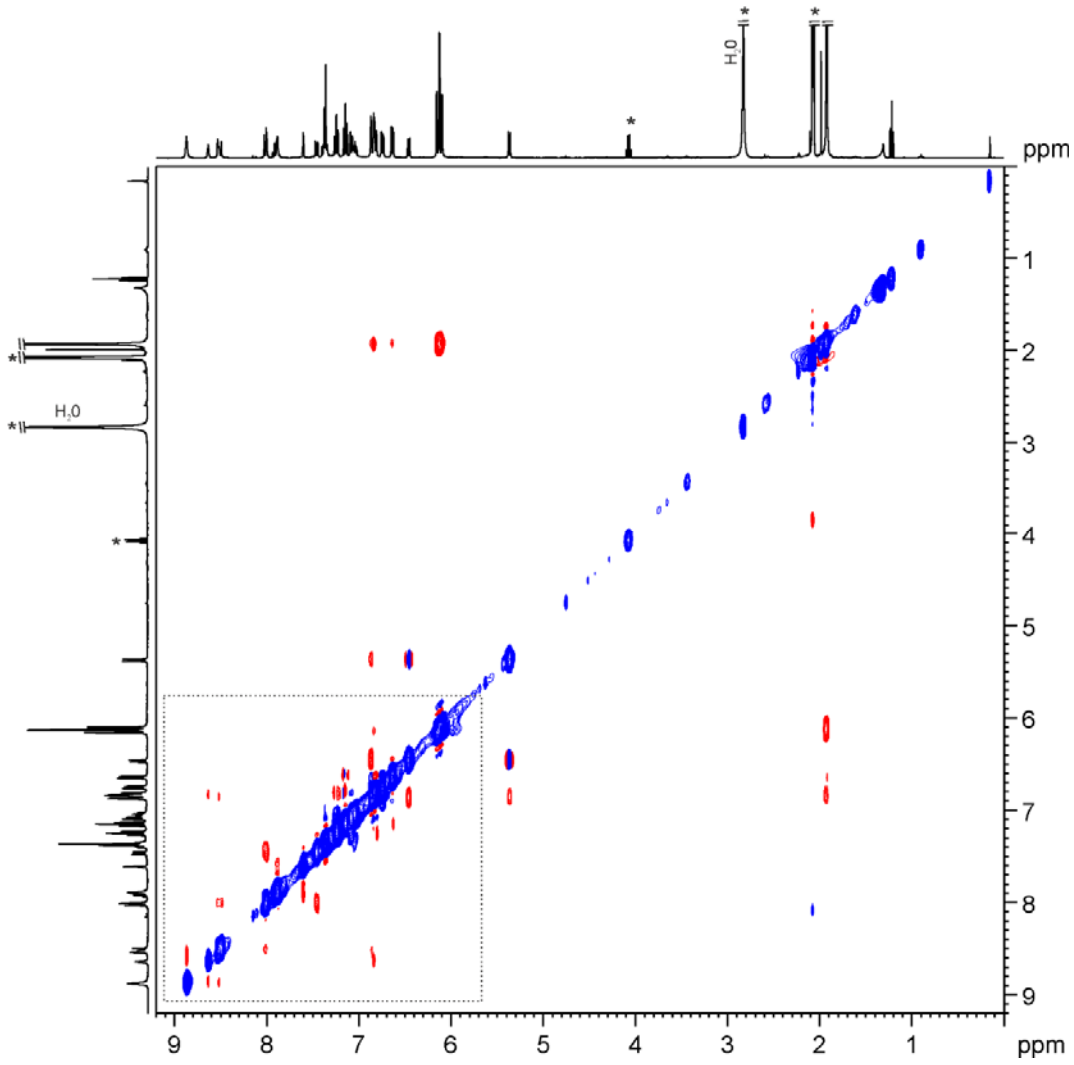

Figure S 10 ROESY NMR (400 MHz, $(CD_3)_2CO$, 298 K) spectrum of the cavitand **1in**. * Residual solvent peak.

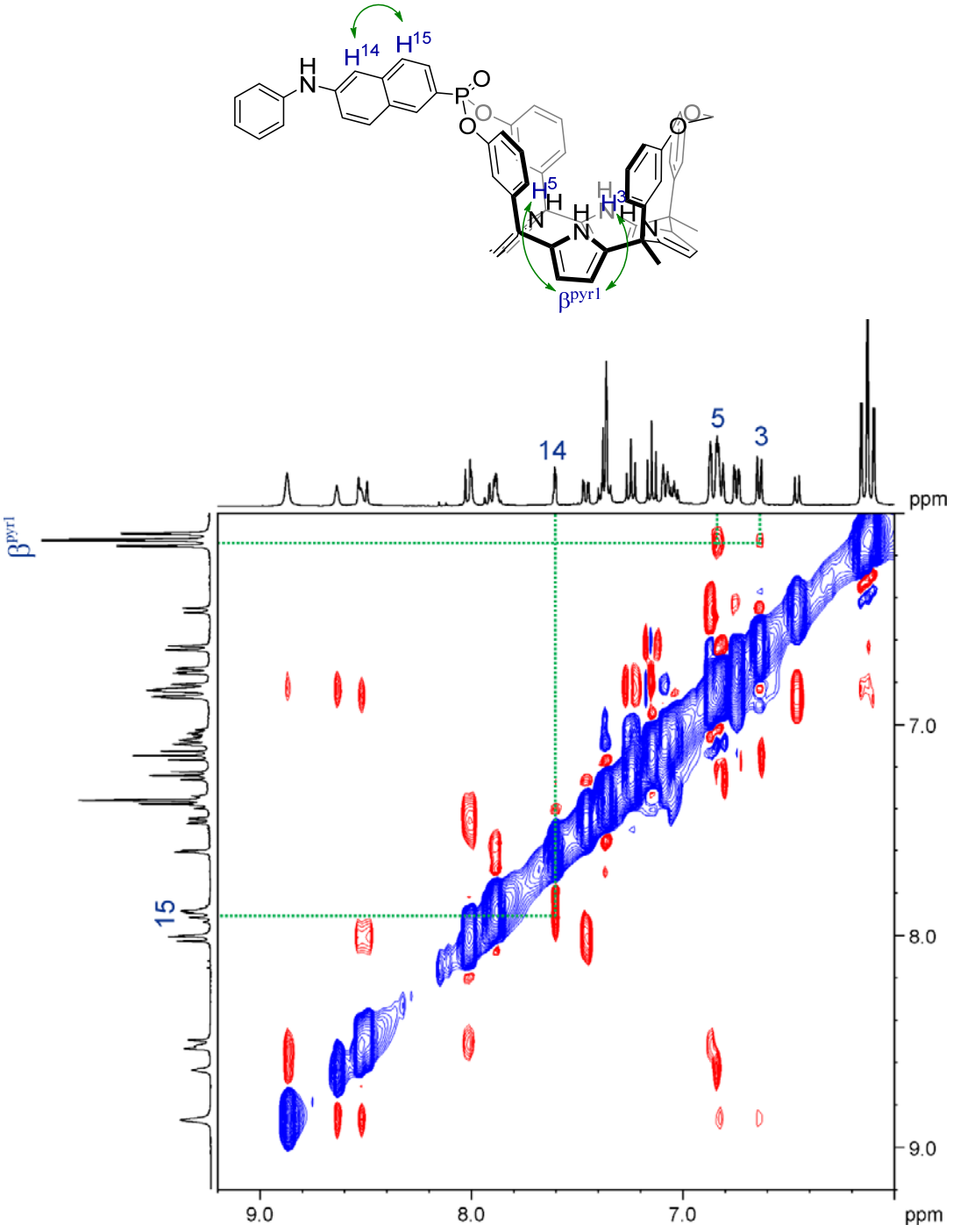

Figure S 11 Expansion of a selected region of the 2D ROESY NMR (400 MHz, $(CD_3)_2CO$, 298 K) spectrum of the cavitand **1in**.

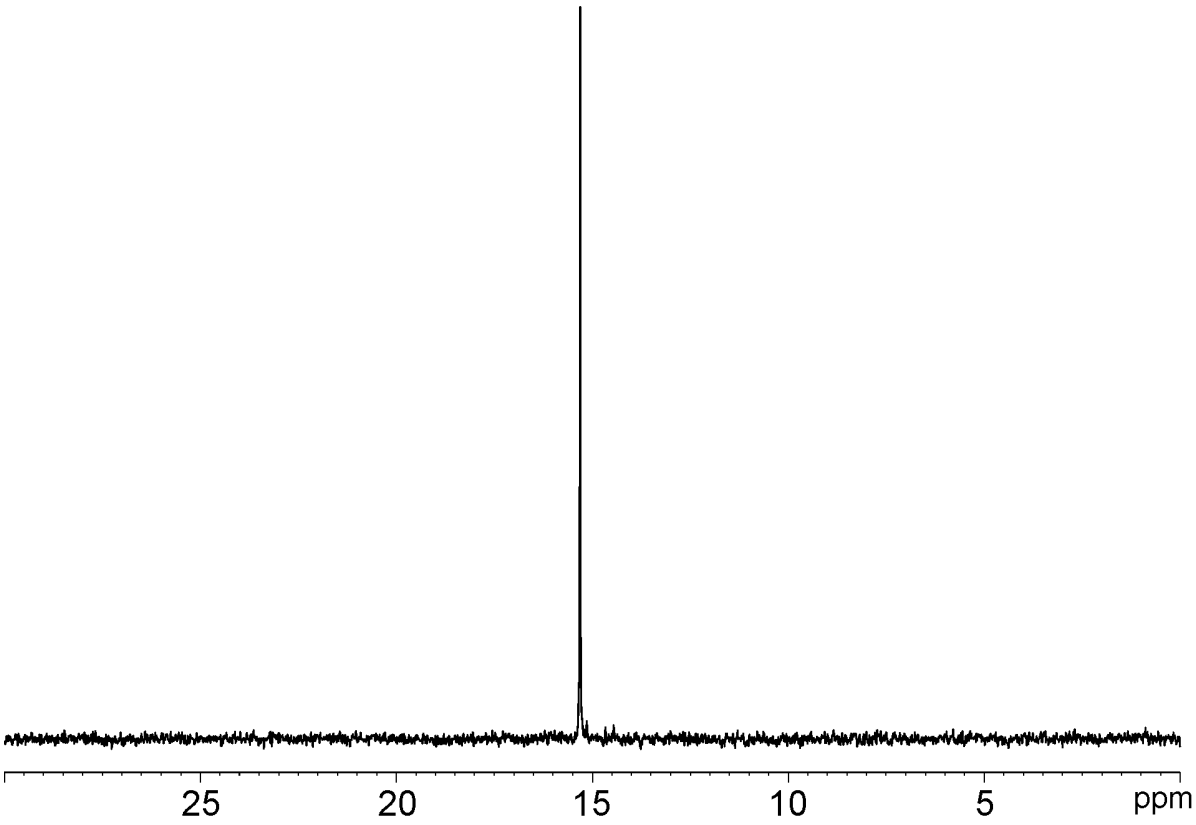

Figure S12 ^{31}P NMR (161 MHz, $(CD_3)_2CO$, 298 K) of cavitand **1in**.

Mono-phosphonate calix[4]pyrrole cavitand 1out

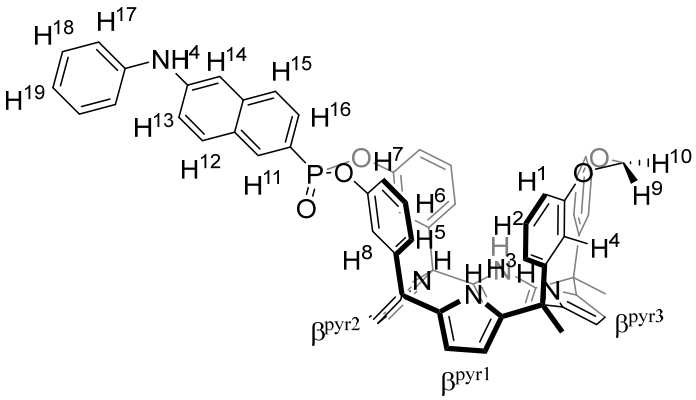

Receptor **1out. Rf**: 0.3 (DCM:AcOEt 98:2, SiO_2). **^{1}H NMR** (400 MHz, $(CD_3)_2CO$, 298 K): δ (ppm) = 8.81 (bs, 2H, NH^1), 8.74 (bs, 1H, NH^2), 8.45 (bs, 1H, NH^3), 8.43 (d, 1H, *J* = 16.38 Hz, H^{11}), 7.98 (bs, 1H, NH^4), 7.97 (d, 1H, *J* = 8.90 Hz, H^{12}), 7.86-7.81 (m, 2H, $H^{15,16}$), 7.61 (s, 2H, H^8), 7.58 (d, 1H, *J* = 2.25 Hz, H^{14}), 7.43 (dd, 1H, J_1 = 8.90 Hz, J_2 = 2.25 Hz, H^{13}), 7.39-7.30 (mult., 4H, H^{17}-H^{18}), 7.22 (t, 2H, *J* = 7.94 Hz, H^6), 7.11 (t, 2H, *J* = 7.94 Hz, H^2), 7.02 (tt, 1H, J_1 = 6.60 Hz, J_2 = 2.05 Hz, H^{19}), 6.88 (dd, 2H, J_1 = 8.35 Hz, J_2 = 2.35 Hz, H^5), 6.82 (s, 2H, H^4), 6.79 (d, 2H, *J* = 7.94 Hz, H^7), 6.71 (dd, 2H, J_1 = 8.35 Hz, J_2 = 2.60 Hz, H^1), 6.65 (d, 2H, *J* = 7.94 Hz, H^3), 6.38 (d, 1H, *J* = 8.02 Hz, H^9), 6.12 (d, 2H, *J* = 2.60 Hz, β^{pyr2}), 6.07 (d, 2H, *J* = 2.60 Hz, β^{pyr3}), 6.05 (d, 4H, *J* = 2.60 Hz, β^{pyr1}), 5.35 (d, 1H, *J* = 8.02 Hz, H^{10}), 1.93 (s, 6H, CH_3), 1.90 (s, 6H, CH_3). **^{31}P-NMR** (161 MHz, $(CD_3)_2CO$, 298 K): δ (ppm) = 14.45.

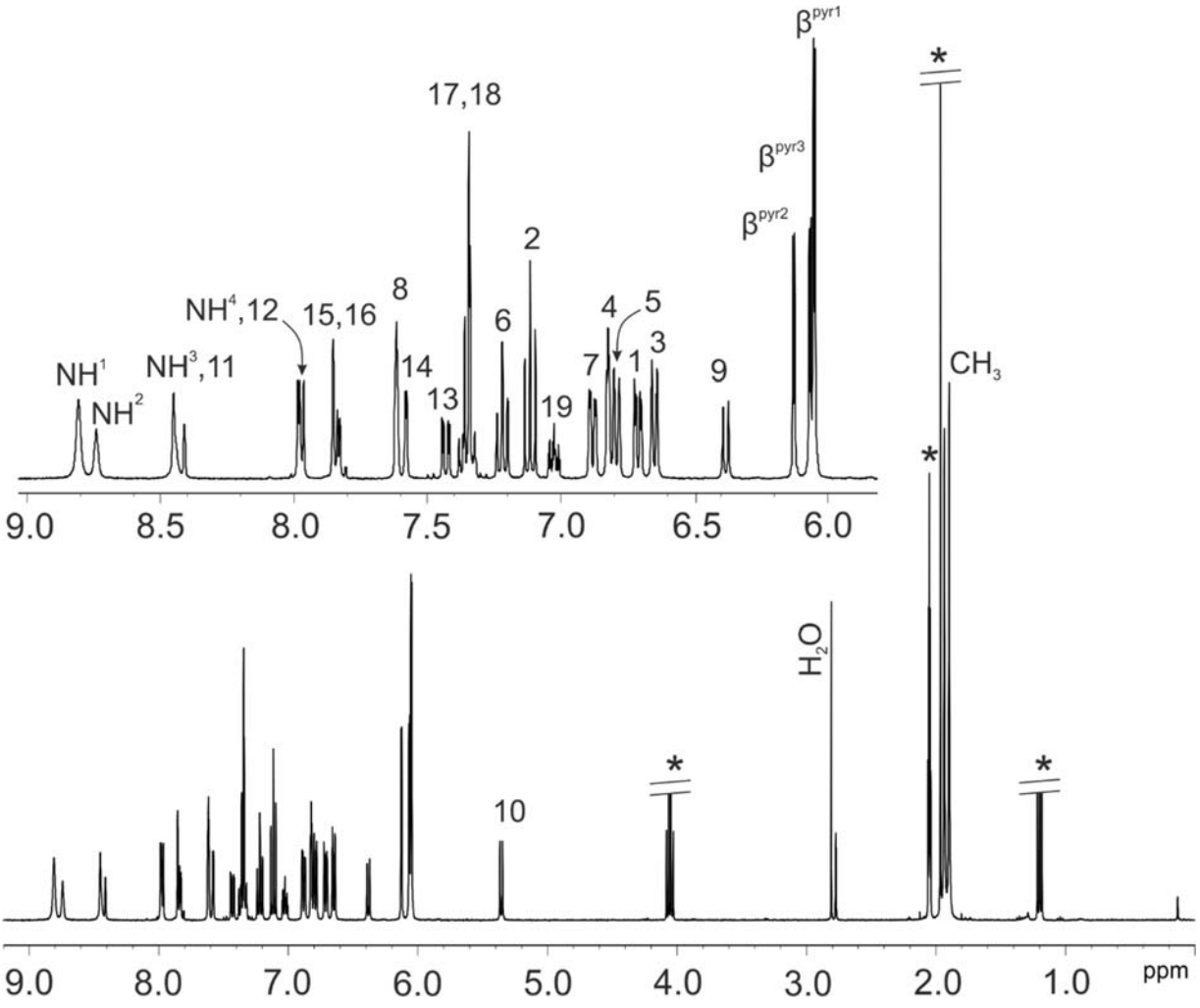

Figure S13 ^{1}H NMR (400 MHz, $(CD_3)_2CO$, 298 K) spectrum of cavitand **1out**.*Residual solvent peak.

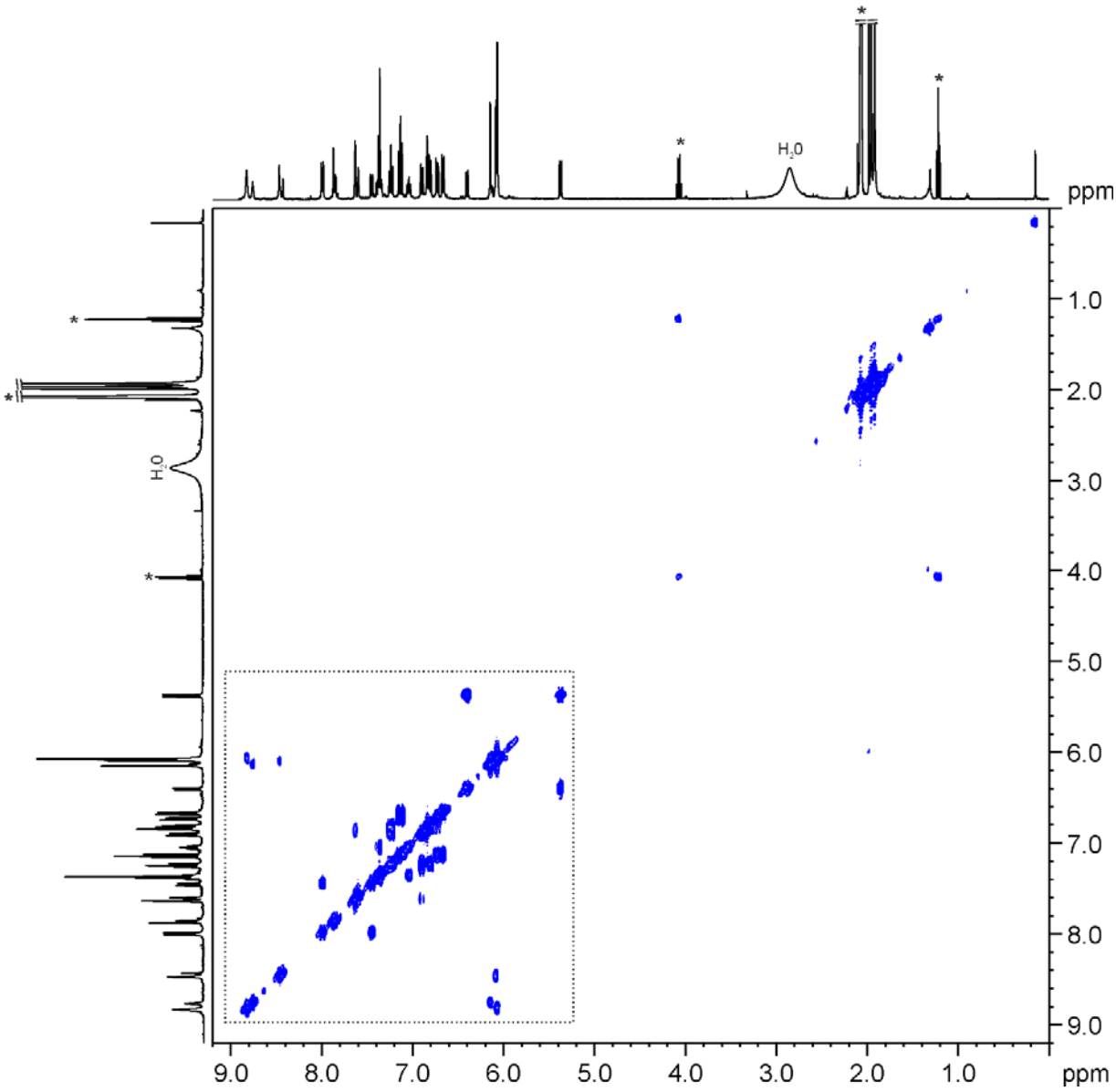

Figure S 14 2D COSY NMR (400 MHz, $(CD_3)_2CO$, 298 K) spectrum of cavitand **1out**. * Residual solvent peak.

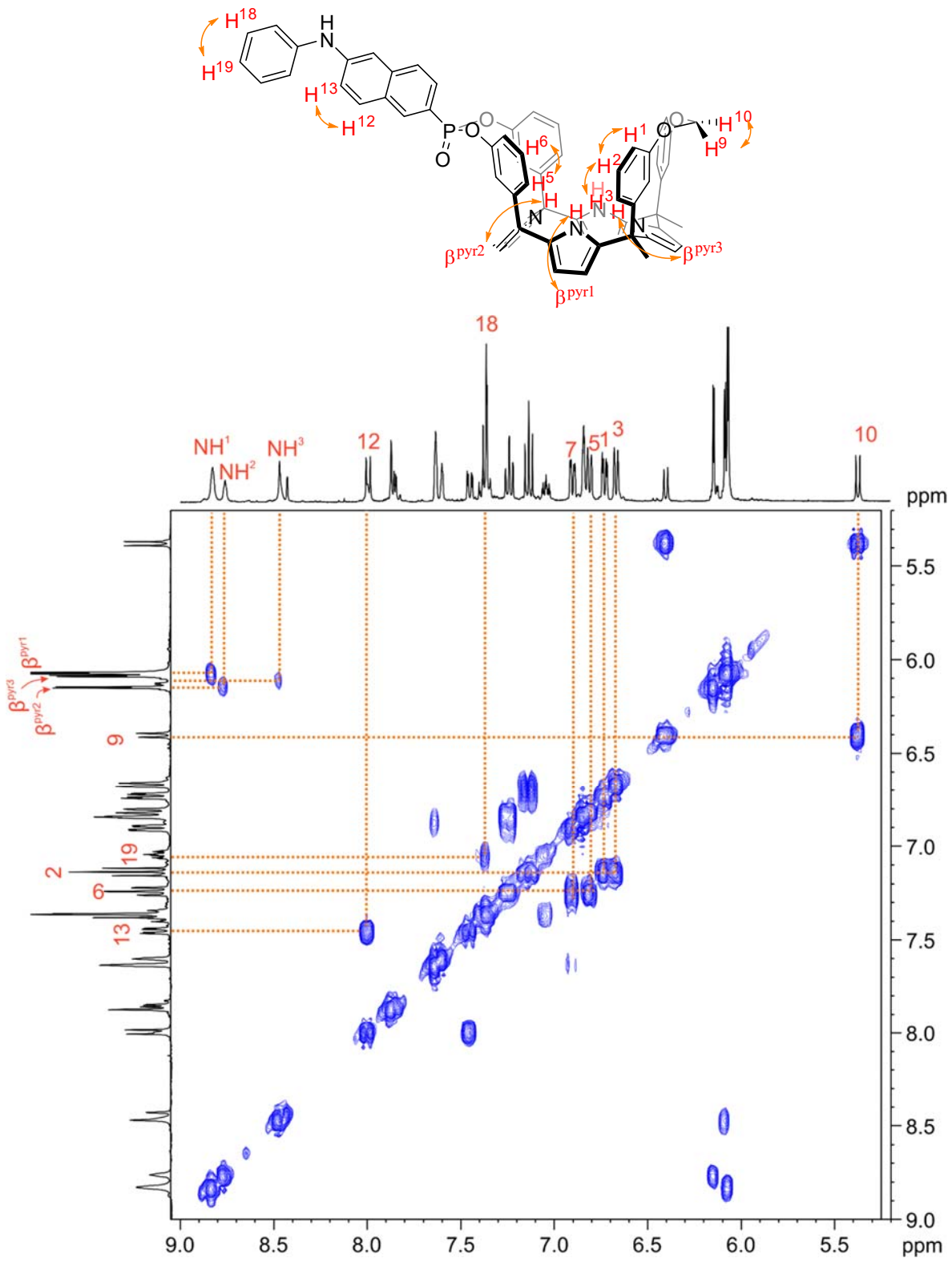

Figure S 15 Expansion of a selected region of the 2D COSY NMR (400 MHz, $(CD_3)_2CO$, 298 K) spectrum of cavitand **1out**.

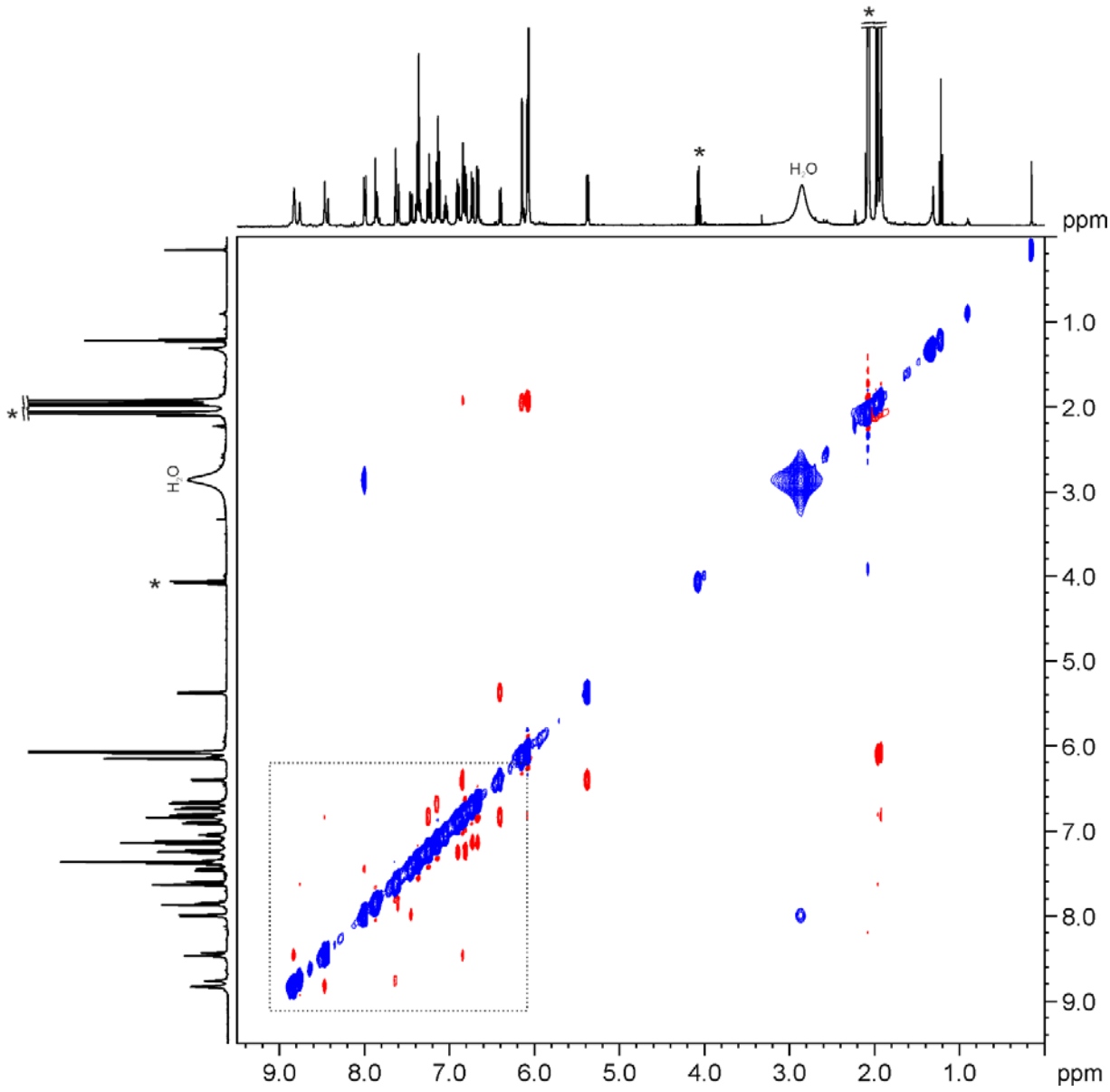

Figure S 16 NOESY NMR (400 MHz, $(CD_3)_2CO$, 298 K) spectrum of cavitand **1out**. * Residual solvent peak.

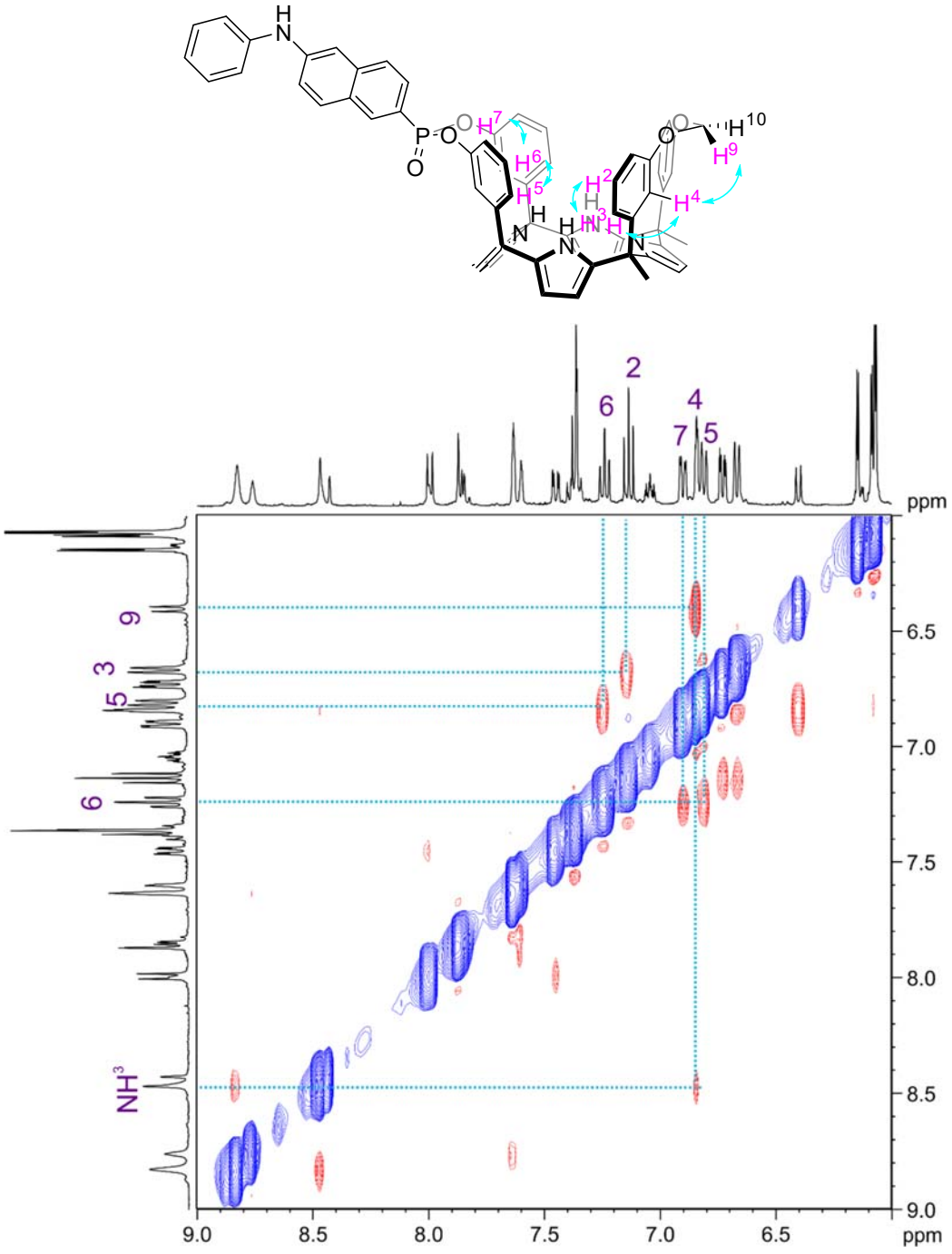

Figure S 17 Expansion of a selected region of the 2D NOESY NMR (400 MHz, $(CD_3)_2CO$, 298 K) spectrum of cavitand **1out**.

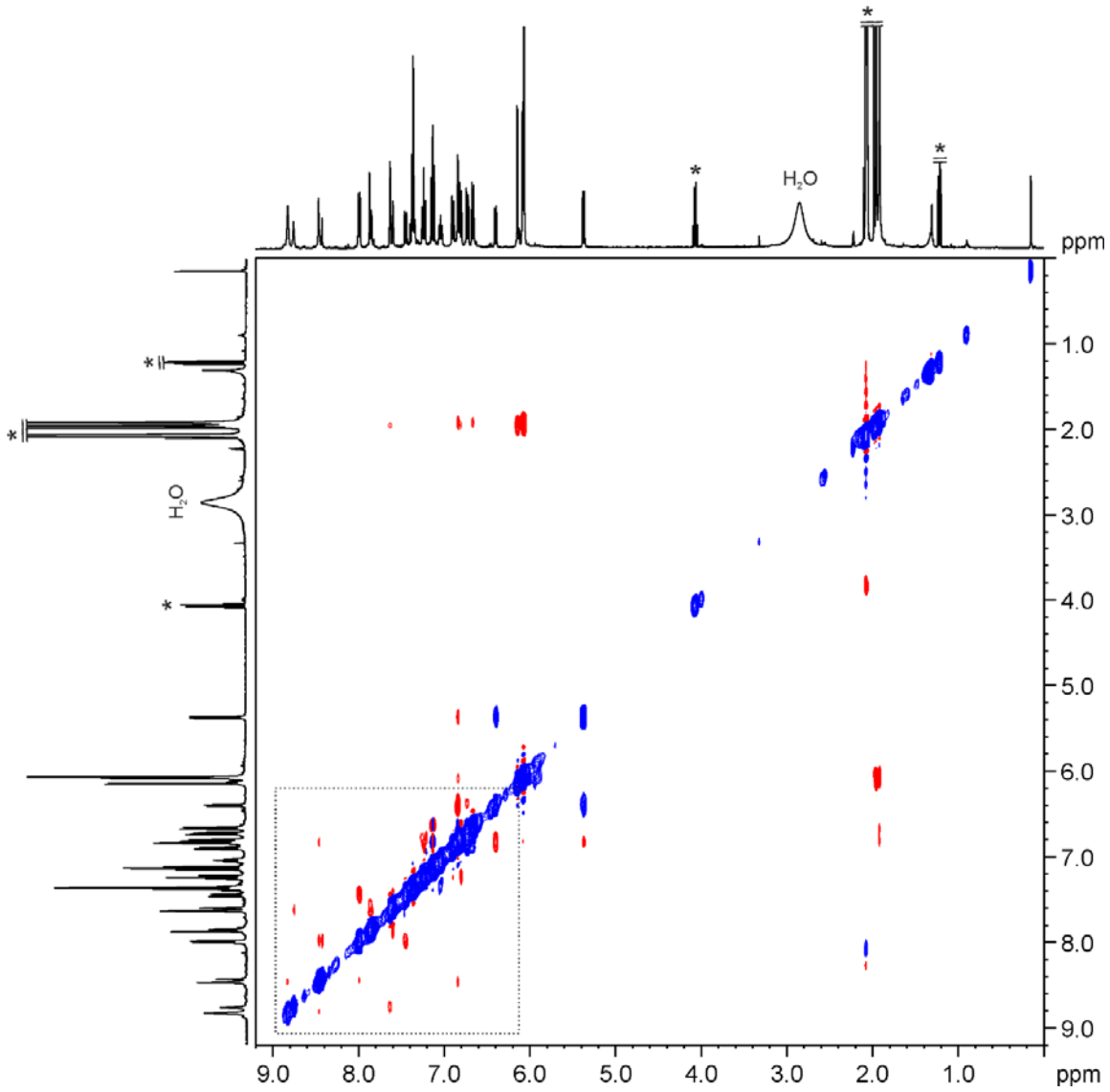

Figure S 18 ROESY NMR (400 MHz, $(CD_3)_2CO$, 298 K) spectrum of the compound **1out**. * Residual solvent peak.

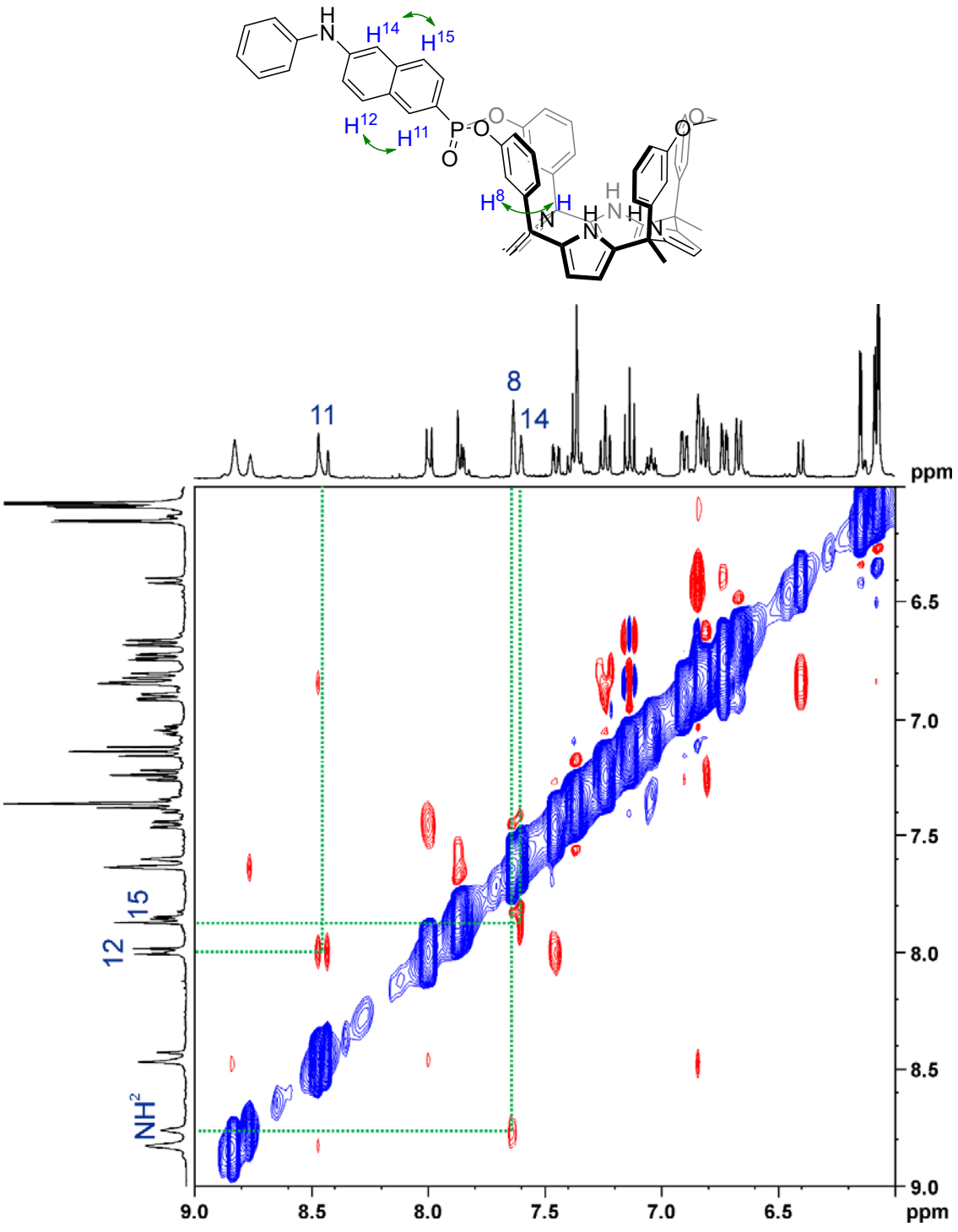

Figure S 19 Expansion of a selected region of the 2D ROESY NMR (400 MHz, $(CD_3)_2CO$, 298 K) spectrum of cavitand **1out**.

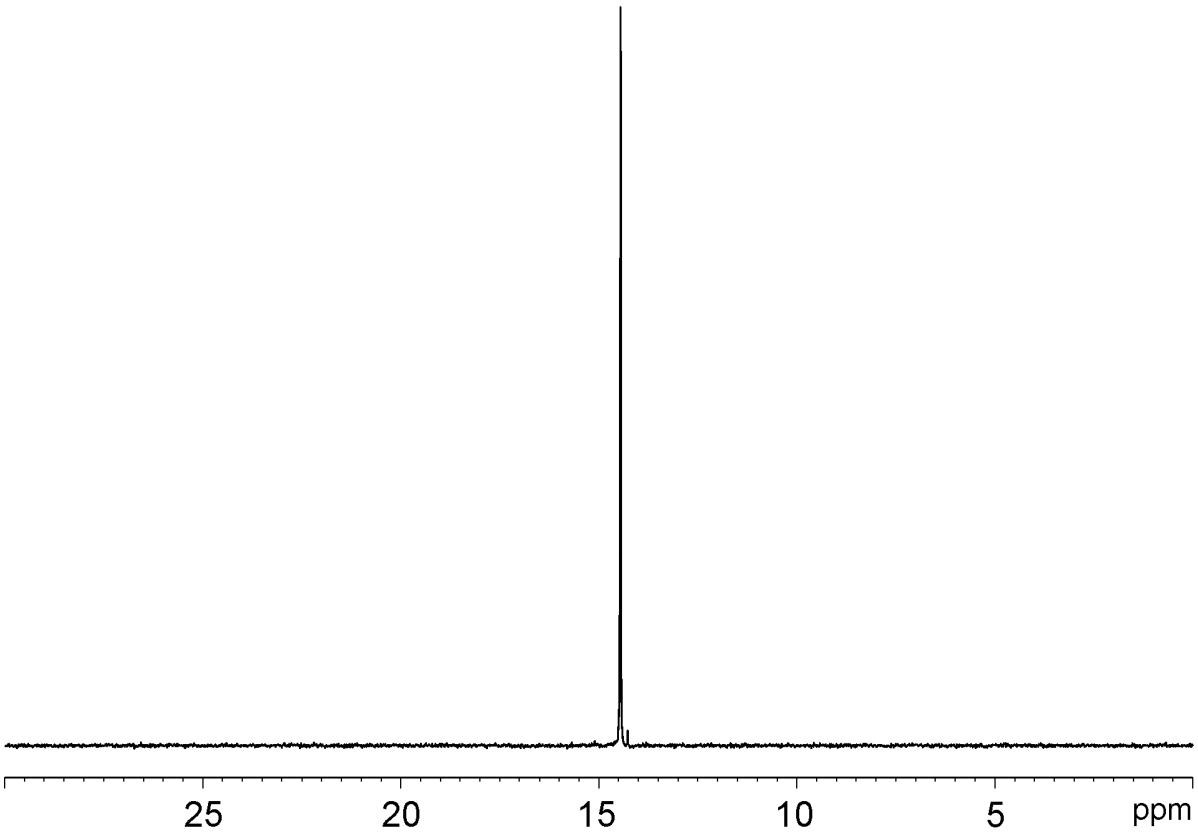

Figure S20 ^{31}P NMR (161 MHz, $(CD_3)_2CO$, 298 K) spectrum of compound **1out**.

2.3 Direct binding-based sensing (BBS) : UV-Vis absorption and emission titrations

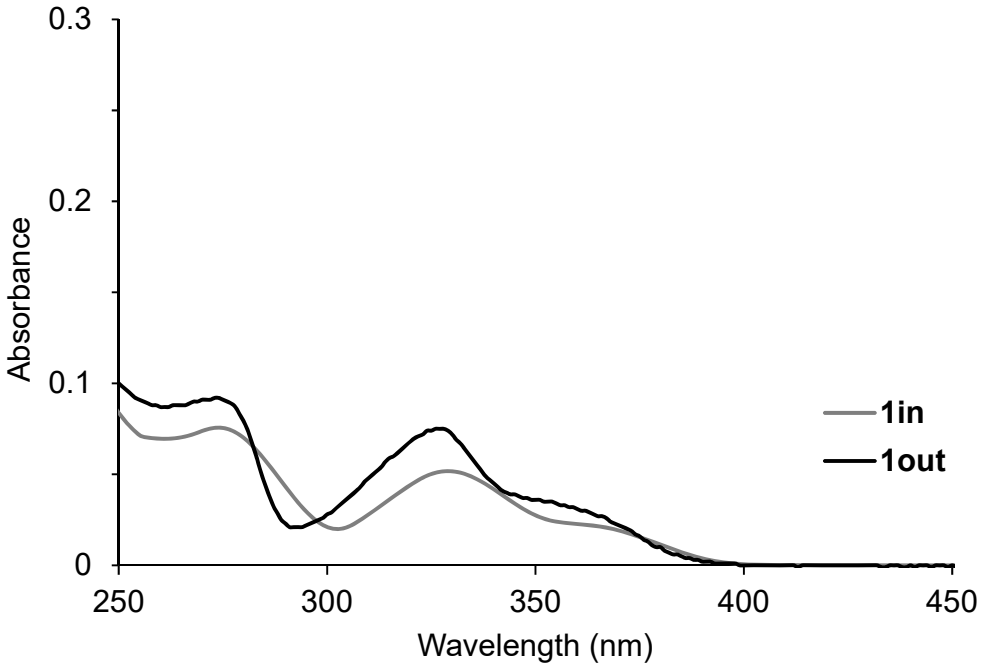

Figure S 21 UV-Vis spectra of a 2.5 µM solution of **1in** (grey line) and **1out** (black line) in DCM.

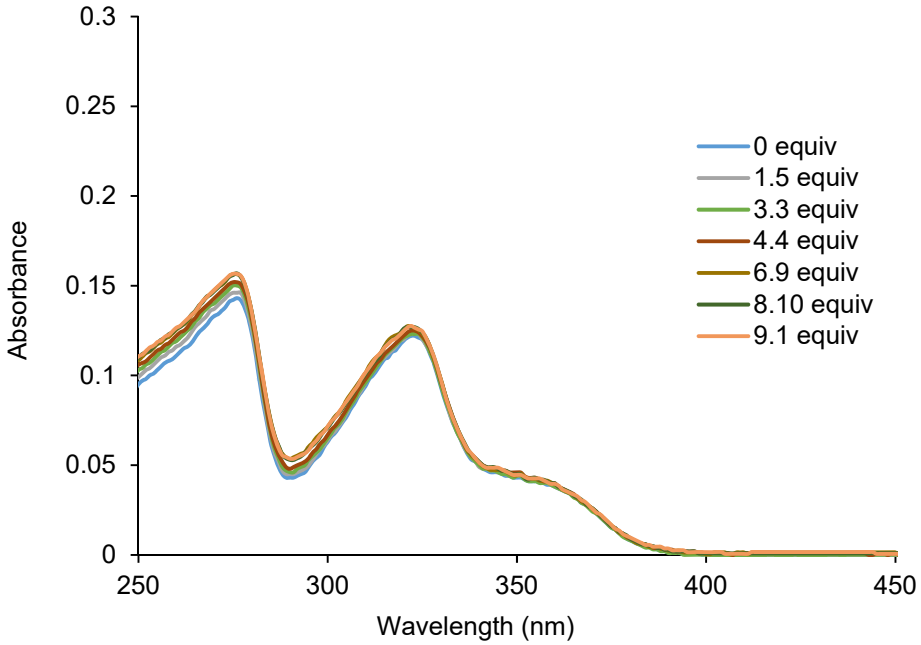

Figure S 22 UV-Vis spectra of a 1 µM solution of **7** in DCM registered during the addition of incremental amounts of L-Pro.

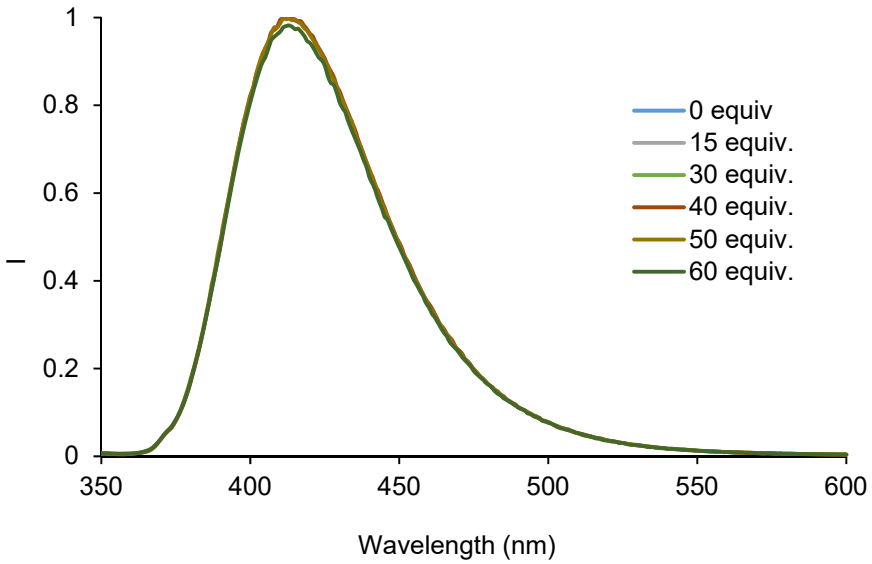

Figure S 23 Normalized emission spectra (λ_{exc} = 335 nm) of **7** (1 µM) in DCM registered during the addition of incremental amounts of L-Pro.

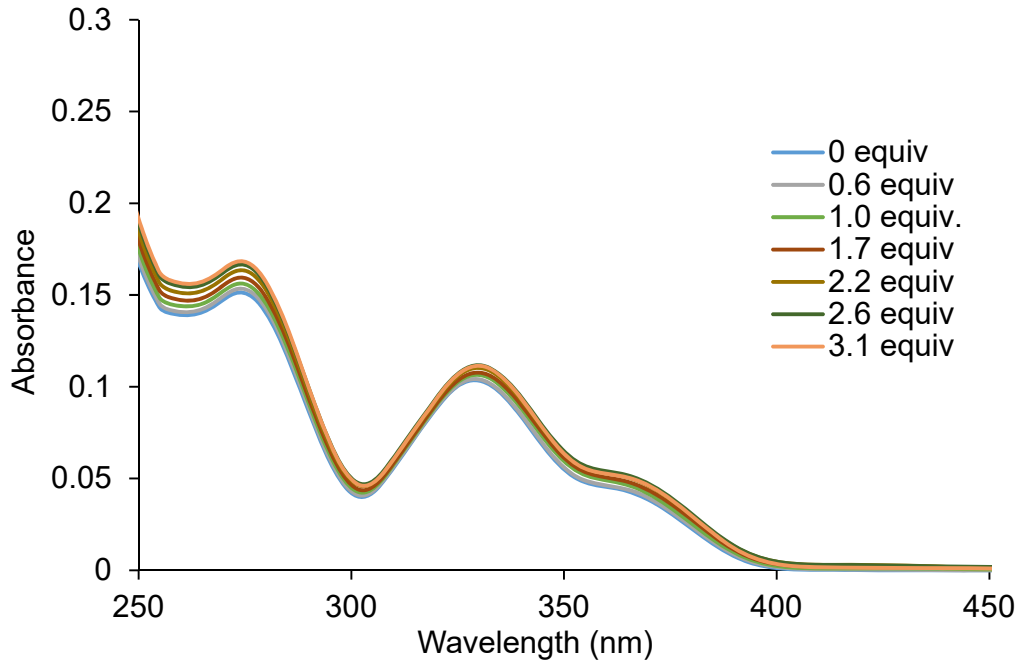

Figure S 24 UV-Vis spectra of a 1 µM solution of **1in** in DCM registered during the addition of incremental amounts of L-Pro.

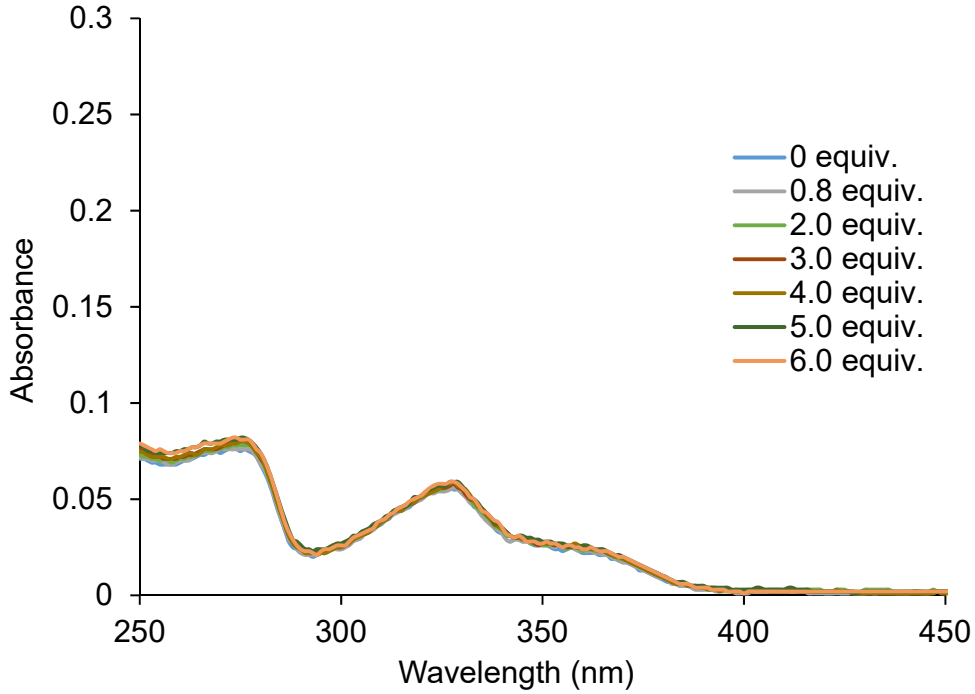

Figure S 25 UV-Vis spectra of a 0.5 µM solution of **1in** in DCM registered during the addition of incremental amounts of L-Pip.

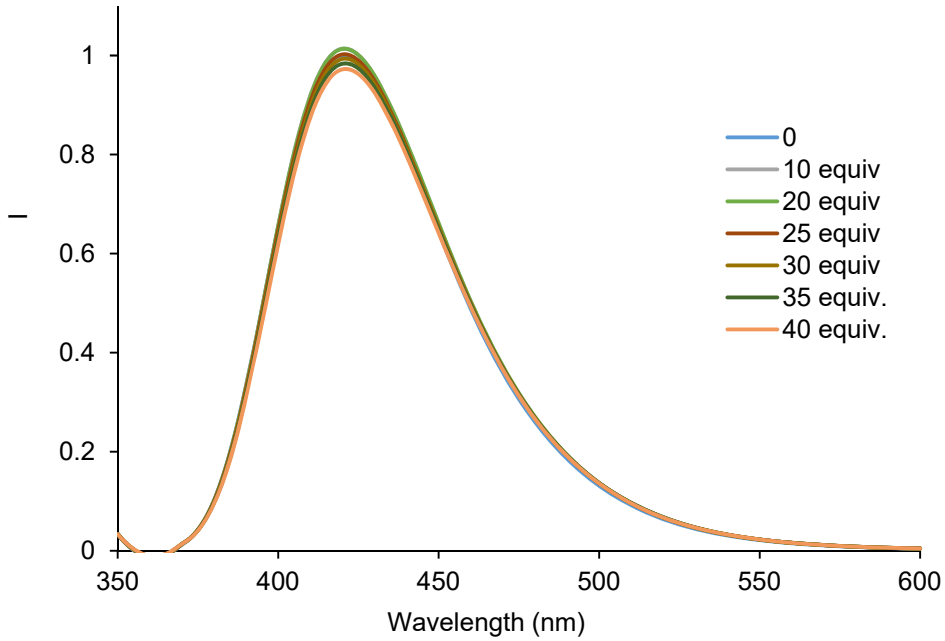

Figure S 26 Normalized emission spectra (λ_{exc} = 335 nm) of **1in** (1 µM) in DCM registered during the addition of incremental amounts of L-Pip.

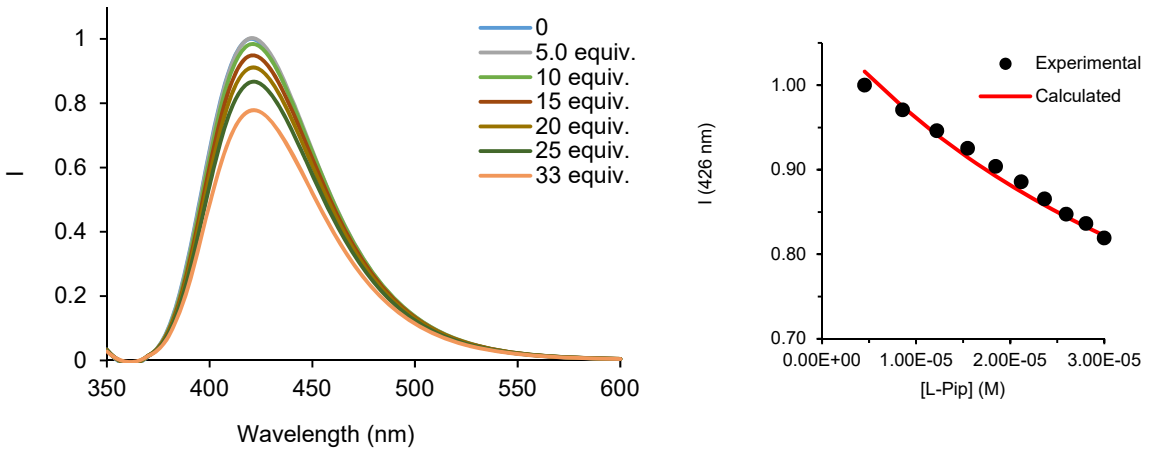

Figure S 27 Left) Normalized emission spectra (λ_{exc} = 335 nm) of **1out** (1 μM) in DCM registered during the addition of incremental amounts of L-Pip. Right) Plot of the emission change at 426 nm (black circles) vs concentration of L-Pip. The red line corresponds to the fit of the titration data.

2.4 FRET-based Indicator Displacement Assays (IDA)

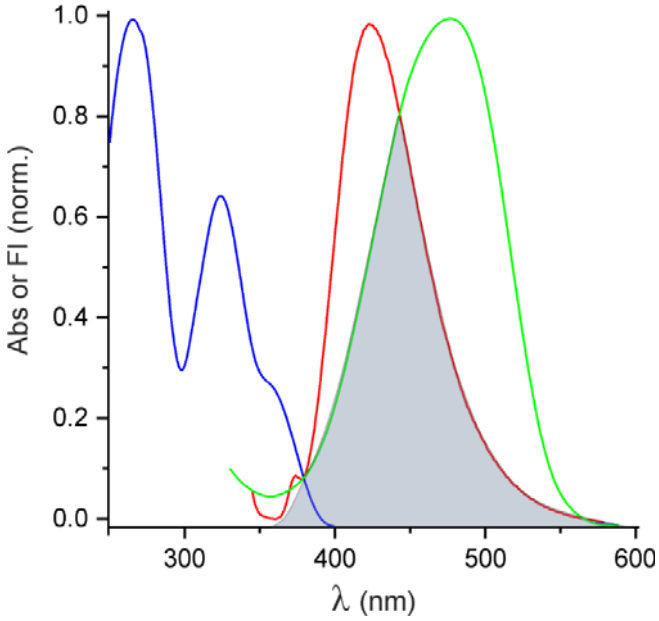

Figure S 28 UV-Vis absorption spectra of **1in** (blue) and **6** (red) and the fluorescence spectrum of **1in** (green). The spectral overlap is highlighted in grey.

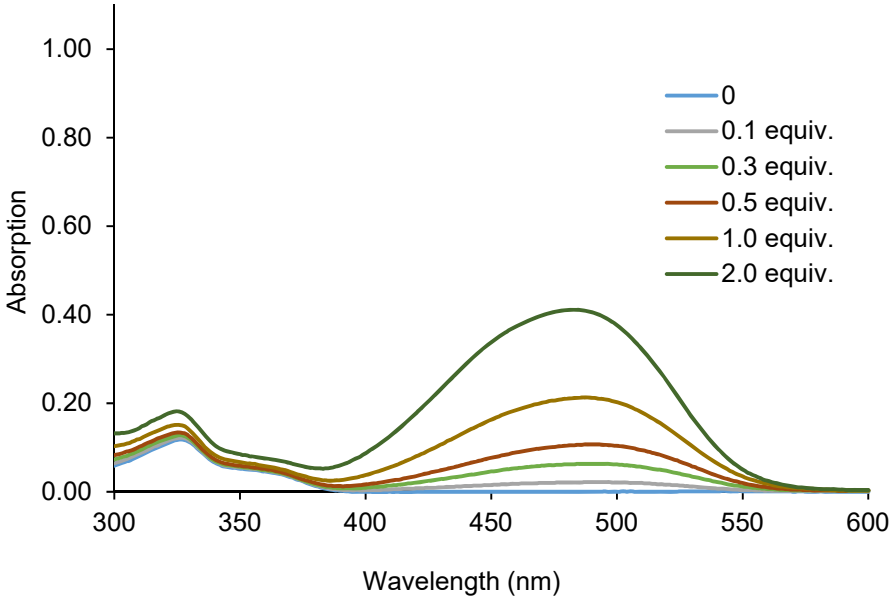

Figure S 29 UV-Vis spectra of a 0.5 µM solution of **1in** in DCM registered during the addition of incremental amounts of **6**.

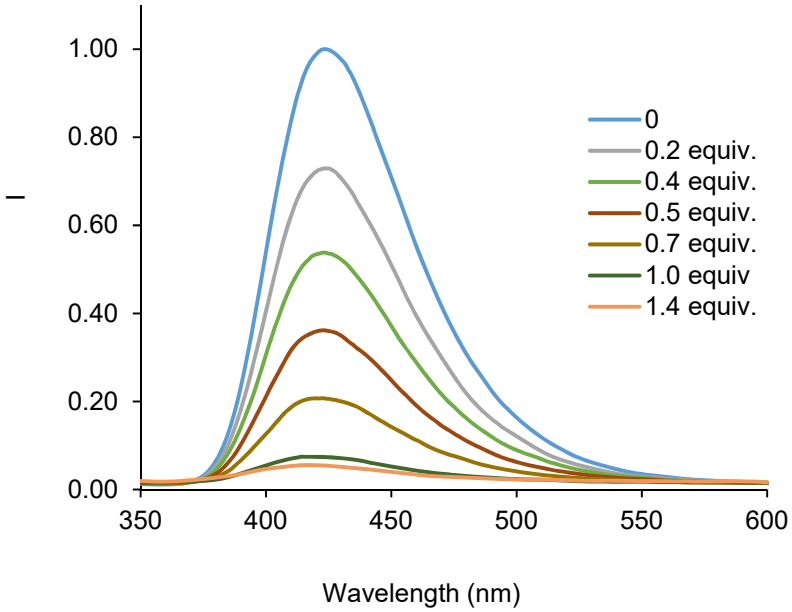

Figure S 30 Normalized emission spectra (λ_{exc} = 335 nm) of **1in** (5 µM) in DCM registered during the addition of incremental amounts of **6**.

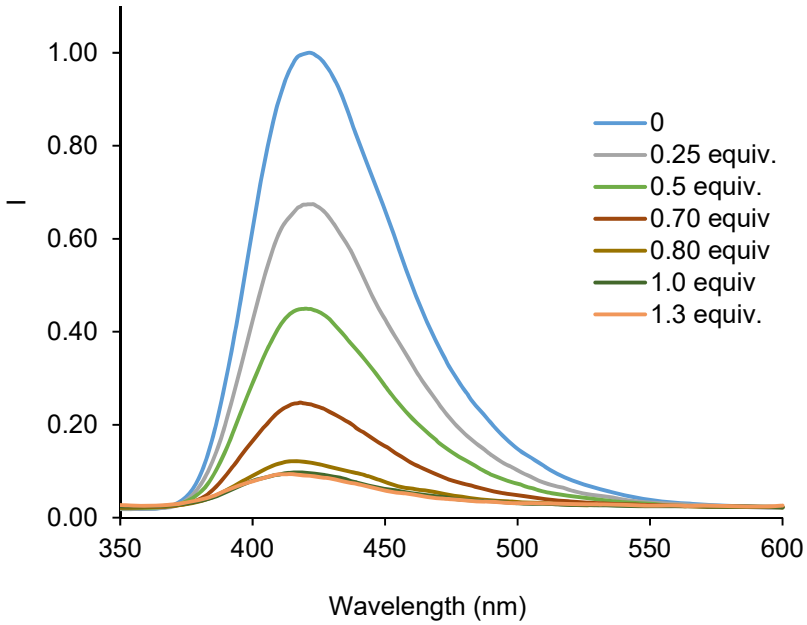

Figure S 31 Normalized emission spectra (λ_{exc} = 335 nm) of **1out** (5 µM) in DCM registered during the addition of incremental amounts of **6**.

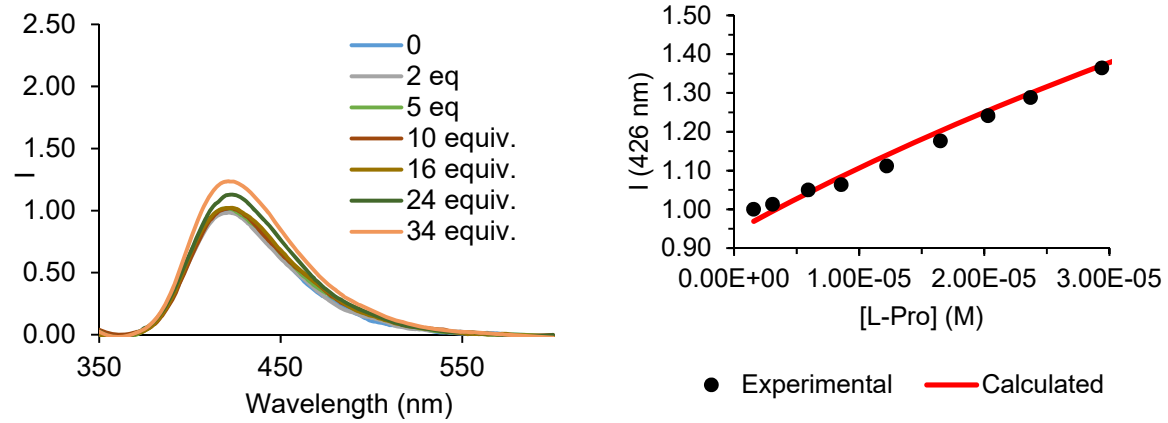

Figure S 32 Left) Normalized emission spectra registered during the competitive IDA experiments of **6⊂1out** complex with incremental addition of L-Pro in dichloromethane solution; λ_{exc} = 335 nm. Right) Plot of the emission change at 426 nm (black circles) vs concentration of L-Pro. The red line corresponds to the fit of the titration data

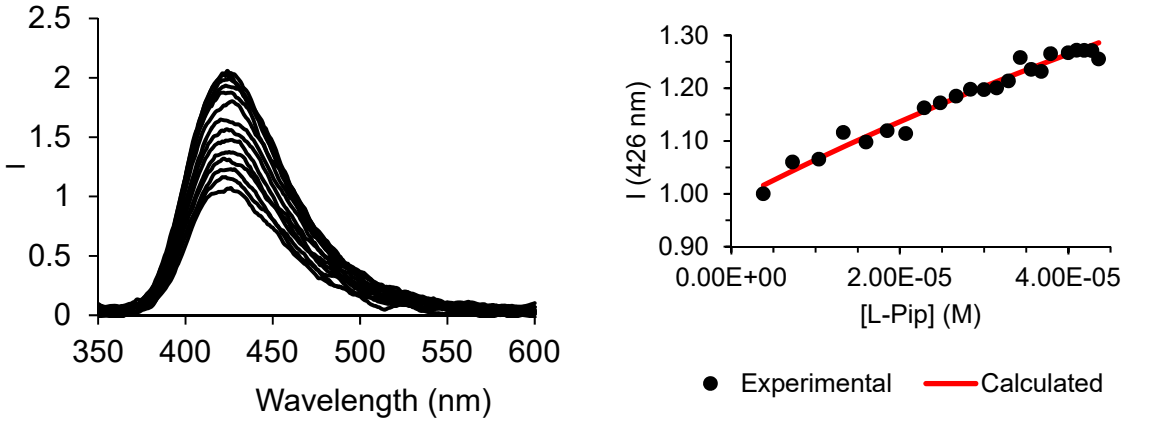

Figure S 33. Left) Normalized emission spectra registered during the competitive IDA experiments of **6⊂1in** complex with incremental addition of L-Pip in dichloromethane solution; λ_{exc} = 335 nm. Right) Plot of the emission change at 426 nm (black circles) vs concentration of L-Pip. The red line corresponds to the fit of the titration data

2.5 Energy minimized structures of inclusion complexes

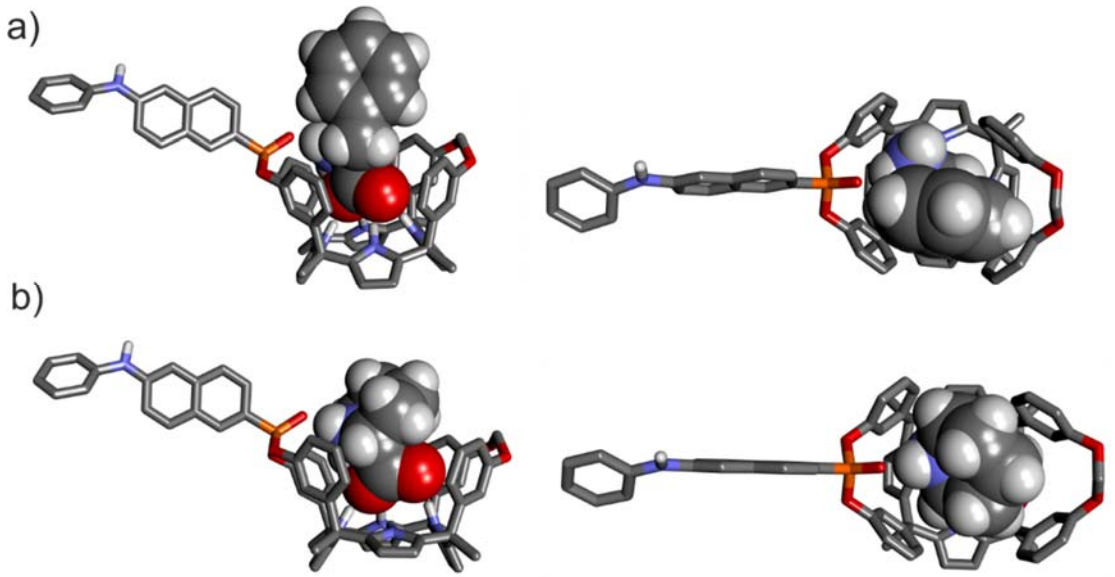

Figure S 34 Side and top views of the energy-minimized inclusion complexes L-Phe⊂**1in** (a) and L-Pip$_{ax}$⊂**1in** (b). The structures are energy minima at the BP86/def2-SVP level of theory. The receptors are shown in stick representation. Non-polar hydrogen atoms of the host were removed for clarity. The included amino acids are depicted as CPK models.

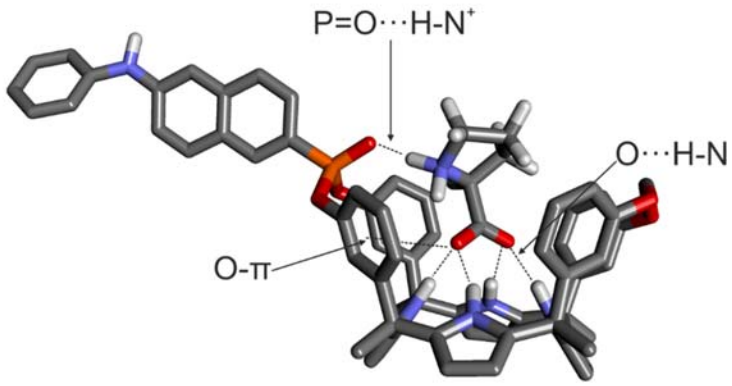

Figure S 35 Side view of the energy-minimized inclusion complex L-Pip$_{eq}$⊂**1in**. Hydrogen bond and O-π interactions are indicated. The structures are energy minima at the BP86/def2-SVP level of theory. The receptor and the included amino acid are shown in stick representation. Non-polar hydrogen atoms of the receptor were removed for clarity.

SI References

[1] T. Guinovart, D. Hernandez-Alonso, L. Adriaenssens, P. Blondeau, M. Martinez-Belmonte, F. X. Rius, F. J. Andrade and P. Ballester, Recognition and Sensing of Creatinine, *Angew. Chem., Int. Ed.*, 2016, **55**, 2435-2440.

[2] J. P. Perdew, Density-functional approximation for the correlation energy of the inhomogeneous electron gas, *Phys. Rev. B*, 1986, **33**, 8822-8824.

[3] A. D. Becke, Density-functional exchange-energy approximation with correct asymptotic behavior, *Phys. Rev. A*, 1988, **38**, 3098-3100.

[4] Gaussian 09, Revision A.02, M. J. Frisch, G. W. Trucks, H. B. Schlegel, G. E. Scuseria, M. A. Robb, J. R. Cheeseman, G. Scalmani, V. Barone, G. A. Petersson, H. Nakatsuji, X. Li, M. Caricato, A. Marenich, J. Bloino, B. G. Janesko, R. Gomperts, B. Mennucci, H. P. Hratchian, J. V. Ortiz, A. F. Izmaylov, J. L. Sonnenberg, D. Williams-Young, F. Ding, F. Lipparini, F. Egidi, J. Goings, B. Peng, A. Petrone, T. Henderson, D. Ranasinghe, V. G. Zakrzewski, J. Gao, N. Rega, G. Zheng, W. Liang, M. Hada, M. Ehara, K. Toyota, R. Fukuda, J. Hasegawa, M. Ishida, T. Nakajima, Y. Honda, O. Kitao, H. Nakai, T. Vreven, K. Throssell, J. A. Montgomery, Jr., J. E. Peralta, F. Ogliaro, M. Bearpark, J. J. Heyd, E. Brothers, K. N. Kudin, V. N. Staroverov, T. Keith, R. Kobayashi, J. Normand, K. Raghavachari, A. Rendell, J. C. Burant, S. S. Iyengar, J. Tomasi, M. Cossi, J. M. Millam, M. Klene, C. Adamo, R. Cammi, J. W. Ochterski, R. L. Martin, K. Morokuma, O. Farkas, J. B. Foresman, and D. J. Fox, Gaussian, Inc., Wallingford CT, 2016.

[5] F. Maffei, P. Betti, D. Genovese, M. Montalti, L. Prodi, R. De Zorzi, S. Geremia and E. Dalcanale, Highly Selective Chemical Vapor Sensing by Molecular Recognition: Specific Detection of C1–C4 Alcohols with a Fluorescent Phosphonate Cavitand, *Angew. Chem., Int. Ed.*, 2011, **50**, 4654-4657.

[6] M. Ciardi, F. Tancini, G. Gil-Ramírez, E. C. Escudero Adán, C. Massera, E. Dalcanale and P. Ballester, Switching from Separated to Contact Ion-Pair Binding Modes with Diastereomeric Calix[4]pyrrole Bis-phosphonate Receptors, *J. Am. Chem. Soc.*, 2012, **134**, 13121-13132.